

A Second-Order TGV Discretization with Some Invariance Properties

Alireza Hosseini^a, Kristian Bredies^b

^a*School of Mathematics, Statistics and Computer Science, University of Tehran, P.O. Box 14115-175, Tehran, Iran. Email: hosseini.alireza@ut.ac.ir*

^b*Institute of Mathematics and Scientific Computing, University of Graz, Heinrichstraße 36, A-8010 Graz, Austria. Email: kristian.bredies@uni-graz.at*

Abstract

In this work, we propose a new discretization for second-order total generalized variation (TGV) with some distinct properties compared to existing discrete formulations. The introduced model is based on same design principles as Condat's discrete total variation model (*SIAM J. Imaging Sci.*, 10(3), 1258–1290, 2017) and shares its benefits, in particular, improved quality for the solution of imaging problems. An algorithm for image denoising with second-order TGV using the new discretization is proposed. Numerical results obtained with this algorithm demonstrate the discretization's advantages. Moreover, in order to compare invariance properties of the new model, an algorithm for calculating the TGV value with respect to the new discretization model is given.

Keywords: Image processing, total generalized variation, TGV discretization, image denoising, primal-dual algorithm.

1. Introduction

Image reconstruction is one of the major subjects in image and signal processing. It can be applied in areas such as medical imaging, pattern recognition, video coding and so on. There are various kinds of techniques for image reconstruction; e.g., spatial filtering [1, 2], transform domain filtering [3, 4, 5], methods which are based on partial differential equations [6, 7] and variational methods [9, 10, 11, 12, 13]. Moreover, methods which are based on machine learning such as deep learning [27, 28], linear regression [29] and so on have received increasing attention. All of these classes of methods are currently areas of active research. In this paper, we contribute to variational methods in order to make progress in this area. In particular, a new kind of discrete variational model is proposed to solve image processing tasks. The proposed model is associated with a new discretization of the so-called second-order total generalized variation (TGV) [13] which is explained below.

In imaging problems, it is common to solve inverse problems. Generally, solving an inverse problem amounts to solving an equation of the form

$$z = G(u),$$

where u is the initial “perfect” image in a continuous domain (e.g., $u \in L^1_{loc}(\Omega)$, for $\Omega \subset \mathbb{R}^d$ domain), G is a forward operator such as blurring, sampling, or more generally, some linear operator, and z is the measured data. The problem is thus reconstructing u from the given data z . Often, such inverse problems are ill-posed, so regularization is necessary. A common regularization approach is Tikhonov regularization which can be formulated as the following optimization problem:

$$\min_u \mathcal{F}(u) + \mathcal{R}(u), \tag{1}$$

where \mathcal{F} represents the data fidelity and \mathcal{R} is the regularization functional. The most common fidelity term is of the form

$$\mathcal{F}(u) = \frac{1}{2} \|G(u) - z\|^2,$$

where $\|\cdot\|$ is a given norm. The regularization functional \mathcal{R} is commonly adapted for imaging problems and the associated applications such as medical imaging, machine vision and so on. Standard Tikhonov regularization approaches will usually consider quadratic forms such as $\mathcal{R}(u) = \frac{1}{2} \|u\|_2^2$ or $\frac{1}{2} \|\nabla u\|_2^2$. However, it is shown in [31], that

for denoising problems, $\mathcal{R}(u) = \frac{1}{2}\|u\|_2^2$ enforces no spatial regularization (i.e., noise removal) of any kind. Therefore, this is an inadequate choice, since all natural images admit a lot of spatial regularity. On the other hand, the second case ($\mathcal{R}(u) = \frac{1}{2}\|\nabla u\|_2^2$), normally imposes too much spatial regularization. In a pioneer work, Rudin, Osher and Fatemi [8] introduced the “Total Variation” (TV) as a regularizer for inverse problems in imaging. This model is very simple, easy to discretize and the obtained numerical results for imaging problems are reliable. For instance, acceptable regularization can be obtained for denoising problems, whereas some artifacts still remain; the so-called staircasing artifacts. For this reason, the TV model have been generalized by the introduction of the “Total Generalized Variation” (TGV) [13]. This leads to the definition of the k -th order TGV (TGV^k), for $k \geq 1$, where TGV^1 coincides with TV up to a positive factor. Second order TGV (TGV^2) is the most commonly used TGV model for imaging problems, and it has better performance for piecewise smooth images compared to TV. In particular, the typical artifacts of the TV model do not appear in the results obtained with TGV regularization.

In order to solve real world problems by means of variational models, we need to compute solutions numerically and it is inevitable to discretize each regularization functional. However, the kind of discretization may impact the quality of the solution and is thus of practical relevance. Based on the definition of the total variation, various kinds of discretization approaches have been proposed in the literature, such as discrete isotropic TV [8] and Condat’s discrete TV [11].

The continuous definition of total variation (see definition of TV in Section 2) has the desirable property of being isotropic, or rotation-invariant, that is, in two dimensions, a rotation of an image in the plane does not change the value of TV. It is natural to expect that the discretized form of the total variation functional is rotation-invariant, at least for the rotation of any integer multiple of 90° . In this respect, isotropic TV is easy and fast for implementation, however, in spite of its name, isotropic TV does not admit this isotropy property.

Recently, some effort was made to improve on this, and some other versions of discrete TV with different properties were introduced, such as upwind TV [9] which is about the discrete coarea formula, Shannon discrete TV [12], Condat’s TV which attempts to improve isotropy [11], an approximation of TV by using nonconforming P1 (Crouzeix–Raviart) finite elements [32], and so on. In particular, Condat [11], proposed a new discretization of TV (TV_c). Since our new proposed discrete TGV model is inspired by Condat’s discretization, we give a brief explanation of this model in the course of this paper. In a nutshell, Condat’s idea is applying the dual formulation of isotropic TV instead of primal one with some additional constraints which result from domain conversion operators. It is shown that the TV_c value is invariant to 90° rotation and for imaging problems such as denoising and upscaling, it admits better performance in comparison to classic discrete isotropic TV. On the other hand, a discretization approach for second-order TGV is given in [13]. This discretization is a straightforward generalization of classic isotropic TV. It is obtained by the straightforward discretization of the dual formulation of the continuous TGV^2 functional (see definition of TGV^2 in Section 2) and we call it classic discrete TGV. To the best knowledge of the authors, more sophisticated discretization strategies appear to be missing in the literature. The contribution of this paper is designing a new discretization of TGV^2 in two dimensions that has some favorable properties compared to the existing standard discretization approaches. As mentioned, for TGV, this standard discretization is via finite difference operators with known drawbacks such as lack of rotational invariance, even for grid preserving 90° rotations. Currently, the design of approaches with more favorable properties is an open problem. The contribution of this paper is towards filling this gap. In particular, we generalize the recently proposed state-of-the-art strategy by Condat [11].

The rest of the paper is organized as follows. Section 2 is a review of TV and TGV functionals, containing definitions and relevant existing discretizations. In Section 3, for designing the new discrete second-order TGV, staggered grid sets as well as some elementary operators are introduced. Then, new difference operators are proposed and together with the domain conversion operators, the mathematical model of the new discrete second-order TGV is formulated. In Section 4, some basic invariance properties of the proposed model are explained. In Section 5, numerical algorithms for the solution of noise removal problems are proposed and the results are compared to classic discrete TV, Condat’s discrete TV and classic discrete TGV. Moreover, the rotation invariance of the new proposed discrete TGV with respect to integer multiples of 90 degree rotations is illustrated numerically and compared to the existing classic discrete TGV model [13].

2. TV, TGV and their discretizations

In the following, we review TV and TGV functionals including two well-known TV discretization models; isotropic TV and Condat's TV as well as the classic TGV discretization.

2.1. Total variation

The total variation (TV) is a prevalent functional which is frequently employed to regularize ill-posed inverse problems in imaging. In continuous domains, the total variation of a $u \in L^1_{loc}(\Omega)$, $\Omega \subset \mathbb{R}^d$ domain is defined by

$$\text{TV}(u) = \sup \left\{ - \int_{\Omega} u \cdot \text{div} \phi \, dX : \phi \in C_c^1(\Omega, \mathbb{R}^d), |\phi(X)| \leq 1 \, \forall X \in \Omega \right\}. \quad (2)$$

For $u \in C^1(\Omega)$ (or $W^{1,1}(\Omega)$), it can be verified that

$$\text{TV}(u) = \int_{\Omega} |\nabla u| \, dX. \quad (3)$$

In this paper, (3) and (2), are referred to the primal and the dual formulation of the TV, respectively.

2.2. Second order TGV

Total generalized variation of order k (TGV^k , $k \in \mathbb{N}$), is a regularization functional which has been introduced in [13]. Also, see [14]-[19] for theoretical aspects and [20]-[26] for applications of TGV. It is a generalization of the total variation functional TV (2) (in the sense of $\text{TGV}^1 = \alpha_0 \text{TV}$). If $k \geq 2$, TGV^k has some exceptional properties, such as attenuating artifacts, especially staircase artifacts in imaging problems which are common for TV regularization. The second-order TGV in the continuous domain is defined by:

$$\text{TGV}_{\alpha}^2(u) = \sup \left\{ \int_{\Omega} u \cdot \text{div}^2 v \, dX : v \in C_c^2(\Omega, \text{Sym}^2(\mathbb{R}^d)), \|\text{div}^l v\|_{\infty} \leq \alpha_l, l = 0, 1 \right\}, \quad (4)$$

for $u \in L^1_{loc}(\Omega)$, $\Omega \subset \mathbb{R}^d$ domain, $\alpha_0 > 0, \alpha_1 > 0$. In the paper, we focus on the two dimensional setting, i.e., $d = 2$. If $u \in C^2(\Omega)$, this definition can be rewritten by

$$\text{TGV}_{\alpha}^2(u) = \min_w \left\{ \alpha_1 \int_{\Omega} |\nabla u - w| \, dX + \alpha_0 \int_{\Omega} |\epsilon(w)| \, dX \right\}, \quad \epsilon(w) = \begin{pmatrix} \frac{\partial w_1}{\partial x} & \frac{\frac{\partial w_1}{\partial y} + \frac{\partial w_2}{\partial x}}{2} \\ \frac{\frac{\partial w_1}{\partial y} + \frac{\partial w_2}{\partial x}}{2} & \frac{\partial w_2}{\partial y} \end{pmatrix}, \quad (5)$$

where $X = (x, y)$. Referring to [13], $C_c^2(\Omega, \text{Sym}^2(\mathbb{R}^2))$ is the set of symmetric $\mathbb{R}^{2 \times 2}$ matrices whose components belong to $C_c^2(\Omega)$. In this paper, (5) and (4), are referred to the primal and the dual formulation of the second-order TGV, respectively.

Remark 2.1. In the above TGV definition, for $d = 2$, $\Omega \subset \mathbb{R}^2$, $u : \Omega \rightarrow \mathbb{R}$, $u \in L^1_{loc}(\Omega)$, $v = \begin{pmatrix} v_1 & v_3 \\ v_3 & v_2 \end{pmatrix}$, $v_1, v_2, v_3 \in C_c^2(\Omega)$. From definition of the divergence in [13], we have

$$\text{div} v = \begin{pmatrix} \frac{\partial v_1}{\partial x} + \frac{\partial v_3}{\partial y} \\ \frac{\partial v_2}{\partial y} + \frac{\partial v_3}{\partial x} \end{pmatrix}. \quad (6)$$

Moreover, for $w = (w_1, w_2)$, $w_1, w_2 \in C_c^1(\Omega)$,

$$\text{div} w = \frac{\partial w_1}{\partial x} + \frac{\partial w_2}{\partial y}, \quad (7)$$

From the fact that $\text{div}^2 v = \text{div}(\text{div} v)$, and definition of $\text{div} v$, it can be easily seen that

$$\text{div}^2 v = \frac{\partial^2 v_1}{\partial x^2} + \frac{\partial^2 v_2}{\partial y^2} + 2 \frac{\partial^2 v_3}{\partial x \partial y}.$$

To discretize TV and TGV, we need some forward difference operators. In the following, let $A = \{1, \dots, N_1\} \times \{1, \dots, N_2\}$. We define the discrete operators:

$D_{x+} : \mathbb{R}^{N_1 \times N_2} \rightarrow \mathbb{R}^{N_1 \times N_2}$ as discrete approximation of the partial derivative with respect to direction x :

$$(D_{x+}u)(n_1, n_2) = \begin{cases} u(n_1 + 1, n_2) - u(n_1, n_2), & (n_1, n_2) \in A \setminus (\{N_1\} \times \{1, 2, \dots, N_2\}), \\ 0, & \text{else,} \end{cases} \quad (8)$$

assuming homogeneous discrete Neumann boundary conditions on $\{N_1\} \times \{1, 2, \dots, N_2\}$, i.e.,

$$u(N_1 + 1, n_2) = u(N_1, n_2), \quad n_2 = 1, \dots, N_2.$$

$D_{y+} : \mathbb{R}^{N_1 \times N_2} \rightarrow \mathbb{R}^{N_1 \times N_2}$ as discrete approximation of the partial derivative with respect to direction y :

$$(D_{y+}u)(n_1, n_2) = \begin{cases} u(n_1, n_2 + 1) - u(n_1, n_2), & (n_1, n_2) \in A \setminus (\{1, 2, \dots, N_1\} \times \{N_2\}), \\ 0, & \text{else,} \end{cases} \quad (9)$$

assuming homogeneous discrete Neumann boundary conditions on $\{1, 2, \dots, N_1\} \times \{N_2\}$, i.e.,

$$u(n_1, N_2 + 1) = u(n_1, N_2), \quad n_1 = 1, \dots, N_1.$$

Moreover, we define $\mathcal{D} = (D_{x+}, D_{y+})$.

2.3. Classic discrete TV (isotropic TV) as a discrete TV which is not isotropic literally

The classic discrete TV, also called isotropic TV, for a discrete image $u \in \mathbb{R}^{N_1 \times N_2}$ is defined by:

$$\text{TV}_i(u) = \sum_{n_1=1}^{N_1} \sum_{n_2=1}^{N_2} \sqrt{(D_{x+}u)(n_1, n_2)^2 + (D_{y+}u)(n_1, n_2)^2}. \quad (10)$$

This definition is inspired from the primal formulation of TV for smooth functions (3), with replacing the differential operators $\frac{\partial u}{\partial x}$ and $\frac{\partial u}{\partial y}$ by finite difference operators D_{x+} and D_{y+} (see (8) and (9)). It is easy to see that classic discrete TV has a dual form which can be implemented by the following optimization problem:

$$\begin{aligned} \text{TV}_i(u) = \max_{v \in (\mathbb{R}^2)^{N_1 \times N_2}} \langle \mathcal{D}u, v \rangle &= \max_{v \in (\mathbb{R}^2)^{N_1 \times N_2}} \sum_{n_1=1}^{N_1} \sum_{n_2=1}^{N_2} (D_{x+}u)(n_1, n_2) \cdot v_1(n_1, n_2) + (D_{y+}u)(n_1, n_2) \cdot v_2(n_1, n_2), \\ \text{subject to } |v(n_1, n_2)| &\leq 1, \quad \forall (n_1, n_2) \in \{1, \dots, N_1\} \times \{1, \dots, N_2\}, \end{aligned} \quad (11)$$

where, for $v \in \mathbb{R}^2$, $|v| = \sqrt{v_1^2 + v_2^2}$. Surprisingly, this discretization is not invariant with respect to 90° rotations. In other words, if $\mathcal{R}_{90}u$ is the 90° rotated version of a discrete image u , then generally $\text{TV}_i(u) \neq \text{TV}_i(\mathcal{R}_{90}u)$. As an example, assume $u \in \mathbb{R}^{2 \times 2}$, $u(1, 1) = 1, u(n_1, n_2) = 0, n_1, n_2 = 1, 2, (n_1, n_2) \neq (1, 1)$, then it is easy to see that $\text{TV}_i(u) = \sqrt{2}$ and $\text{TV}_i(\mathcal{R}_{90}u) = 2$. For a general angle θ using the rotation operator \mathcal{R}_θ , we get non-invariance as well. However, the question may arise here what kind of rotation invariance can we expect from a discretization? In the sequel, we review Condat's discrete TV, which is a modified model which is designed by means of grid domain conversions. This discretization is exact up to numerical precision with respect to 90° rotations and gives a better approximation for the other rotation angles in comparison to TV_i .

2.4. Condat's TV as a more isotropic discrete TV

Based on the dual formulation of the continuous TV (2) (whose discretization is given in (11)) and introducing three linear operators $L_\bullet, L_{\leftrightarrow}$ and L_\updownarrow over $(\mathbb{R}^2)^{N_1 \times N_2}$, Condat [11] proposed a new discretization of total variation:

$$\begin{aligned} \text{TV}_c(u) = \max_{v \in (\mathbb{R}^2)^{N_1 \times N_2}} \langle \mathcal{D}u, v \rangle &= \max_{v \in (\mathbb{R}^2)^{N_1 \times N_2}} \sum_{n_1=1}^{N_1} \sum_{n_2=1}^{N_2} (D_{x+}u)(n_1, n_2) \cdot v_1(n_1, n_2) + (D_{y+}u)(n_1, n_2) \cdot v_2(n_1, n_2), \\ \text{subject to } |L_\bullet v(n_1, n_2)| &\leq 1, |L_{\leftrightarrow} v(n_1, n_2)| \leq 1, |L_\updownarrow v(n_1, n_2)| \leq 1, \quad \forall (n_1, n_2) \in \{1, \dots, N_1\} \times \{1, \dots, N_2\}, \end{aligned} \quad (12)$$

where

$$\begin{aligned}
(L_{\bullet}v)_1(n_1, n_2) &= \frac{1}{2}(v_1(n_1, n_2) + v_1(n_1 - 1, n_2)), \quad (L_{\bullet}v)_2(n_1, n_2) = \frac{1}{2}(v_2(n_1, n_2) + v_2(n_1, n_2 - 1)), \\
(L_{\leftrightarrow}v)_1(n_1, n_2) &= \frac{1}{4}(v_1(n_1, n_2) + v_1(n_1 - 1, n_2) + v_1(n_1, n_2 + 1) + v_1(n_1 - 1, n_2 + 1)), \quad (L_{\leftrightarrow}v)_2(n_1, n_2) = v_2(n_1, n_2), \\
(L_{\updownarrow}v)_1(n_1, n_2) &= v_1(n_1, n_2), \quad (L_{\updownarrow}v)_2(n_1, n_2) = \frac{1}{4}(v_2(n_1, n_2) + v_2(n_1, n_2 - 1) + v_2(n_1 + 1, n_2) + v_2(n_1 + 1, n_2 - 1)),
\end{aligned} \tag{13}$$

with zero boundary condition assumptions, that is, for any $(n_1, n_2) \in \{1, 2, \dots, N_1\} \times \{1, 2, \dots, N_2\}$, $v_1(0, n_2) = v_2(n_1, 0) = v_1(N_1, n_2) = v_2(n_1, N_2) = 0$. We also set $(L_{\leftrightarrow}v)_1(N_1, n_2) = (L_{\leftrightarrow}v)_2(N_1, n_2) = 0$, $(L_{\updownarrow}v)_1(n_1, N_2) = (L_{\updownarrow}v)_2(n_1, N_2) = 0$.

From the fact that in the continuous definition (11), the dual variable is bounded everywhere, by inserting three constraints using the proposed linear operators, the dual variables will be imposed to be bounded on a grid three times more dense than the pixel grid. Condat's TV is a discrete TV with some isotropy properties, in other words, after rotating the image by any integer multiple of 90° , the TV value will remain unchanged up to numerical precision and for other rotation angles, a better approximation can be obtained compared to isotropic TV. Moreover, this model is performing well in removing noise and reconstructing edges in comparison to isotropic TV.

The following is concerned with the generalization of this idea to design a discrete second-order total generalized variation with the same rotational invariance properties.

2.5. Classic discrete TGV (discretization of (5))

To our best knowledge, there is only one classic discretization of the second-order TGV [13] which is briefly explained in the following. Assume that $u \in \mathbb{R}^{N_1 \times N_2}$ is a two-dimensional $N_1 \times N_2$ pixels image with homogeneous discrete Neumann boundary conditions, that is $u(n_1, N_2 + 1) = u(n_1, N_2)$, $u(n_1, 0) = u(n_1, 1)$, for $1 \leq n_1 \leq N_1$ and $u(N_1 + 1, n_2) = u(N_1, n_2)$, $u(0, n_2) = u(1, n_2)$, for $1 \leq n_2 \leq N_2$. In the following, based on forward operators introduced in (8) and (9), by enforcing a discrete Gauss–Green theorem, backward operators are defined as well. Consequently, all discrete operators for designing discrete TGV models will be obtained.

It is natural to define $\mathcal{D} = (D_{x+} \ D_{y+}) : \mathbb{R}^{N_1 \times N_2} \rightarrow (\mathbb{R}^2)^{N_1 \times N_2}$, as a discretization of the gradient operator ∇ appearing in (5). Now, we define backward difference operators $D_{x-}, D_{y-} : \mathbb{R}^{N_1 \times N_2} \rightarrow \mathbb{R}^{N_1 \times N_2}$. Note that from the theory of linear operators (the discrete Gauss–Green theorem), for any $u \in \mathbb{R}^{N_1 \times N_2}$, $v \in (\mathbb{R}^2)^{N_1 \times N_2}$, we have:

$$\langle \mathcal{D}u, v \rangle = \langle u, \mathcal{D}^*v \rangle. \tag{14}$$

On the other hand, for $u \in C_0^1(\Omega, \mathbb{R})$ and $v \in C_0^1(\Omega, \mathbb{R}^2)$, $\Omega \subset \mathbb{R}^2$ domain, we have:

$$\langle \nabla u, v \rangle = \int_{\Omega} \nabla u \cdot v \, dx dy = - \int_{\Omega} u \cdot \operatorname{div} v \, dx dy = - \langle u, \operatorname{div} v \rangle, \tag{15}$$

that is, $\nabla^* = -\operatorname{div}$. As \mathcal{D} is a discrete approximation of ∇ , we can define the divergence operator on $(\mathbb{R}^2)^{N_1 \times N_2}$ by $\operatorname{div} = -\mathcal{D}^*$. From (14), we get

$$-\operatorname{div} v = \mathcal{D}^*v = -D_{x-}v_1 - D_{y-}v_2, \tag{16}$$

where for $w \in (\mathbb{R})^{N_1 \times N_2}$, the backward operator D_{x-} in the direction x is given as

$$(D_{x-}w)(n_1, n_2) = w(n_1, n_2) - w(n_1 - 1, n_2), \quad (n_1, n_2) \in A \setminus (\{1, N_1\} \times \{1, \dots, N_2\}).$$

With homogeneous Neumann boundary conditions and the definition of the adjoint operator we get

$$(D_{x-}w)(1, n_2) = w(1, n_2), \quad (D_{x-}w)(N_1, n_2) = -w(N_1 - 1, n_2), \quad n_2 = 1, \dots, N_2.$$

Similarly, the backward operator D_{y-} in the direction y is given as:

$$(D_{y-}w)(n_1, n_2) = w(n_1, n_2 - 1) - w(n_1, n_2), \quad (n_1, n_2) \in A \setminus (\{1, \dots, N_1\} \times \{1, N_2\}),$$

and

$$(D_{y-}w)(n_1, 1) = w(n_1, 1), \quad (D_{y-}w)(n_1, N_2) = -w(n_1, N_2 - 1), \quad n_1 = 1, \dots, N_1.$$

The classic discretization of TGV is the discretization of the continuous version (5) as follows:

$$\begin{aligned} \text{TGV}_\alpha^2(u) = & \min_{w=(w_1, w_2) \in (\mathbb{R}^2)^{N_1 \times N_2}} \alpha_1 \sum_{n_1, n_2} \sqrt{((D_{x+}u)(n_1, n_2) - w_1(n_1, n_2))^2 + ((D_{y+}u)(n_1, n_2) - w_2(n_1, n_2))^2} \\ & + \alpha_0 \sum_{n_1, n_2} \sqrt{(D_{x+}w_1)(n_1, n_2)^2 + (D_{y+}w_2)(n_1, n_2)^2 + \frac{1}{2}[(D_{x+}w_2)(n_1, n_2) + (D_{y+}w_1)(n_1, n_2)]^2}, \end{aligned} \quad (17)$$

where $\alpha_0 > 0$, $\alpha_1 > 0$. The previously introduced operators are sufficient to model this optimization problem.

2.5.1. Dual form of the classic discrete second-order TGV

Here we give the dual formulation of the second-order discrete TGV (17). The operator div , operating on $v \in (\mathbb{R}^2)^{N_1 \times N_2}$ is defined in (16). However, we also need the discrete operator div which operates on $v = \begin{pmatrix} v_1 & v_3 \\ v_3 & v_2 \end{pmatrix} \in S(\mathbb{R}^4)^{N_1 \times N_2}$, where $S(\mathbb{R}^4)^{N_1 \times N_2}$ is the set of symmetric second-order tensor fields in $(\mathbb{R}^4)^{N_1 \times N_2}$. From the definition of div in (6), we can define

$$\text{div} : S(\mathbb{R}^4)^{N_1 \times N_2} \rightarrow (\mathbb{R}^2)^{N_1 \times N_2}, \quad \text{div } v = \begin{pmatrix} D_{x-}v_1 + D_{y-}v_3 \\ D_{x-}v_3 + D_{y-}v_2 \end{pmatrix}. \quad (18)$$

Note that in the following, it is always clear from the context which of the two divergence operators is meant such that using the same notation does not lead to confusion. It can now be checked that div according to (18) is the negative adjoint of \mathcal{E} , where $\mathcal{E} : u \in (\mathbb{R}^2)^{N_1 \times N_2} \rightarrow S(\mathbb{R}^4)^{N_1 \times N_2}$ is given by

$$\mathcal{E}u = \begin{pmatrix} D_{x+}u_1 & \frac{1}{2}(D_{y+}u_1 + D_{x+}u_2) \\ \frac{1}{2}(D_{y+}u_1 + D_{x+}u_2) & D_{y+}u_2 \end{pmatrix}.$$

Furthermore, from the fact that for $v \in C_c^2(\Omega, \text{Sym}^2(\mathbb{R}^d))$, $\text{div}^2 v = \text{div}(\text{div } v)$, we can concatenate the operations in (16) and (18) to obtain a discrete second-order divergence as follows:

$$\begin{aligned} \text{div}^2 : S(\mathbb{R}^4)^{N_1 \times N_2} &\rightarrow \mathbb{R}^{N_1 \times N_2}, \\ \text{div}^2 v &= \text{div } \text{div } v = D_{x-}D_{x-}v_1 + D_{y-}D_{y-}v_2 + [D_{x-}D_{y-} + D_{y-}D_{x-}]v_3. \end{aligned} \quad (19)$$

For the adjoint operator of div^2 , which is the second derivative, i.e., $\mathcal{D}^2 = \mathcal{E}\mathcal{D}$, it is easy to see that

$$u \in (\mathbb{R})^{N_1 \times N_2}, \quad \mathcal{D}^2 u = \begin{pmatrix} D_{x+}D_{x+}u & \frac{1}{2}(D_{y+}D_{x+}u + D_{x+}D_{y+}u) \\ \frac{1}{2}(D_{y+}D_{x+}u + D_{x+}D_{y+}u) & D_{y+}D_{y+}u \end{pmatrix}. \quad (20)$$

Indeed, a discrete Gauss–Green theorem as follows is valid for $u \in \mathbb{R}^{N_1 \times N_2}$ and $v \in S(\mathbb{R}^4)^{N_1 \times N_2}$:

$$\langle u, \text{div}^2 v \rangle = -\langle \mathcal{D}u, \text{div } v \rangle = \langle \mathcal{D}^2 u, v \rangle. \quad (21)$$

Consequently, it can be verified that the Fenchel–Rockafellar dual form of the second order classic discrete TGV (17) is as follows:

$$\text{TGV}_\alpha^2(u) = \max \left\{ \langle u, \text{div}^2 v \rangle : v \in S(\mathbb{R}^4)^{N_1 \times N_2}, |(\text{div}^l v)(n_1, n_2)| \leq \alpha_l \forall (n_1, n_2) \in A, l = 0, 1 \right\}, \quad (22)$$

where for $v \in S(\mathbb{R}^4)$, $|v| = \sqrt{v_1^2 + v_2^2 + 2v_3^2}$. Similar to classic discrete TV, classic discrete TGV suffers from non-invariance with respect to 90° rotations. To compensate this shortcoming, inspired by Condat’s idea, in our proposed model, the dual formulation (instead of the primal one) of the continuous TGV model is considered for discretization. In addition, some bounding constraints based on domain conversion operators are proposed to enhance rotational invariance properties. The new proposed model has the advantages of both Condat’s discrete TV and classic discrete TGV simultaneously, that is, it can attenuate staircase artifacts which is one of the important properties of classic discrete TGV as well as remove noise, reconstruct edges and admit some isotropy properties.

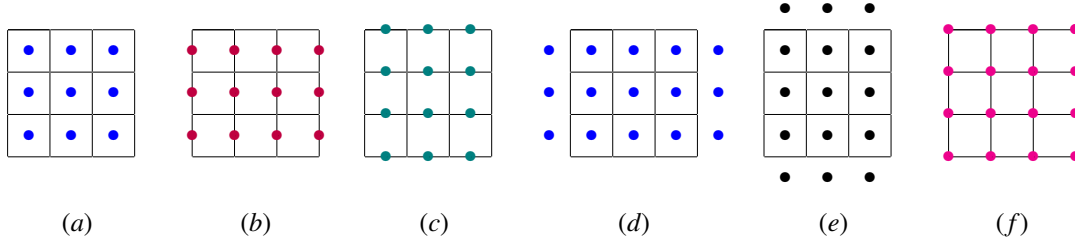


Figure 1: Illustration of the grid sets introduced in Definition 3.1: (a) A_{\bullet} , (b) A_{\leftrightarrow} , (c) A_{\uparrow} , (d) \bar{A}_{\bullet}^x , (e) \bar{A}_{\bullet}^y , (f) A_{\times} .

3. The proposed discretization of the second-order TGV

In order to set up the new discrete TGV functional, we first discuss the required “building blocks”.

1. *Staggered grid domains of the discrete images*: Staggered grids are defined. These sets are essential to define the elementary operators required by the new discrete TGV.
2. *Partial difference operators*: For a given image defined on a staggered grid domain, we explain how we determine the staggered grid domain for the images that result from applying operators to the given image. Consequently, differentiation operators on different staggered grid domains are defined, in particular primal first- and second-order discrete derivatives (\mathcal{D}^{new} , \mathcal{E}^{new} , \mathcal{D}^{2new}). Boundary conditions and grid domains of the images resulting from the new primal operators are determined.
3. *Dual difference operators*: The negative adjoint operators of (\mathcal{D}^{new} , \mathcal{E}^{new} , \mathcal{D}^{2new}) which are first- and second-order divergence operators (div^{new} , div^{2new}) are derived by enforcing a discrete Gauss–Green theorem. In particular, the associated boundary conditions and grid domains for the images resulting from the new dual operators are determined.
4. *Grid interpolation*: In order to design a discretization for TGV with some rotational invariance properties, domain conversion operators are defined. Staggered grid domains and boundary conditions of images obtained from these operators and their duals are studied.
5. *Proposed model and its Fenchel–Rockafellar dual*: The new proposed discrete TGV model is formulated. For this model, a dual formulation is given.

The “building blocks” will be realized in the following.

3.1. Staggered grid domains of the discrete images

We start with introducing the relevant staggered grid sets.

Definition 3.1. For $N_1, N_2 \in \mathbb{N}$, we define the following grid sets:

1. $A_{\bullet} = \{1, \dots, N_1\} \times \{1, \dots, N_2\}$,
2. $A_{\leftrightarrow} = \{\frac{1}{2}, \frac{3}{2}, \dots, N_1 + \frac{1}{2}\} \times \{1, \dots, N_2\}$,
3. $A_{\uparrow} = \{1, \dots, N_1\} \times \{\frac{1}{2}, \frac{3}{2}, \dots, N_2 + \frac{1}{2}\}$,
4. $\bar{A}_{\bullet}^x = \{0, 1, \dots, N_1, N_1 + 1\} \times \{1, \dots, N_2\}$,
5. $\bar{A}_{\bullet}^y = \{1, \dots, N_1\} \times \{0, 1, \dots, N_2, N_2 + 1\}$,
6. $A_{\times} = \{\frac{1}{2}, \frac{3}{2}, \dots, N_1 + \frac{1}{2}\} \times \{\frac{1}{2}, \frac{3}{2}, \dots, N_2 + \frac{1}{2}\}$.

See Figure 1 for an illustration. Moreover, we define the following spaces of discrete functions:

$$\begin{aligned} \mathcal{U}_{\bullet} &= \{u : A_{\bullet} \rightarrow \mathbb{R}\}, & \mathcal{U}_{\leftrightarrow} &= \{u : A_{\leftrightarrow} \rightarrow \mathbb{R}\}, & \mathcal{U}_{\uparrow} &= \{u : A_{\uparrow} \rightarrow \mathbb{R}\}, \\ \bar{\mathcal{U}}_{\bullet}^x &= \{u : \bar{A}_{\bullet}^x \rightarrow \mathbb{R}\}, & \bar{\mathcal{U}}_{\bullet}^y &= \{u : \bar{A}_{\bullet}^y \rightarrow \mathbb{R}\}, & \mathcal{U}_{\times} &= \{u : A_{\times} \rightarrow \mathbb{R}\}. \end{aligned}$$

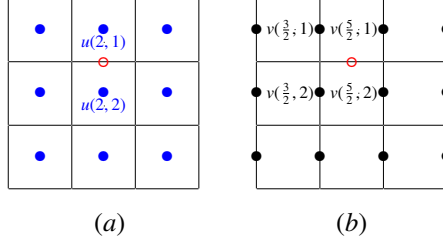


Figure 2: Illustration of Example 3.4: (a) Grid domain of $u : A_{\bullet} \rightarrow \mathbb{R}$. The location of $u(2, 2) - u(1, 2)$ is marked by a red circle. (b) Grid domain of $v : A_{\leftrightarrow} \rightarrow \mathbb{R}$. The location of $\frac{1}{4} \left(v(1, \frac{3}{2}) + v(1, \frac{5}{2}) + v(2, \frac{3}{2}) + v(2, \frac{5}{2}) \right)$ is marked by a red circle.

3.2. Finite difference operators

In the following, differentiation and averaging techniques to determine the grid domain of an image are introduced. The techniques are applied to obtain grid domains of finite difference operators which are essential to design the new discrete TGV in the sequel.

3.2.1. Principles to assign suitable grids as domains for discrete images

Hereafter, we assume the domain of a given discrete image $u \in \mathbb{R}^{N_1 \times N_2}$ is A_{\bullet} . In the other words $u : A_{\bullet} \rightarrow \mathbb{R}$. The domain of discrete images which are obtained from some linear operators could be determined based on two principles; numerical approximation of derivatives and averaging via convex combinations of some objects. We state these two principles with some examples, which are essential for the sequel of the paper. The first principle allows us to find natural discrete domains for the images which are obtained by derivative operators such as $\mathcal{D}, \mathcal{E}, \text{div}, \mathcal{D}^2, \text{div}^2$ (see definitions of these operators in Subsection 2.5). The second principle allows us to define grid domains associated with averaging operators, such as $L_{\bullet}, L_{\leftrightarrow}$ and L_{\uparrow} (these operators will be defined in Subsection 3.4). We need both principles for determining correct grid domains. They are explained in the following:

Principle 3.2. (Numerical differentiation) *The location associated with the difference of two elements in a grid is the center of the locations of these two elements. In other words, the associated grid point for $u(n_1, n_2) - u(m_1, m_2)$ is $(\frac{n_1+m_1}{2}, \frac{n_2+m_2}{2})$.*

Principle 3.3. (Numerical integration and averaging): *The convex combination of elements in some grid domains is located at the respective convex combination of the element's locations. In other words, the vector $\sum_{j=1}^k \alpha_j u(n_1^j, n_2^j)$, $\alpha_j \geq 0, \sum_j \alpha_j = 1$, is associated with the grid point $\sum_{j=1}^k \alpha_j (n_1^j, n_2^j)$.*

Example 3.4. Suppose $u : A_{\bullet} \rightarrow \mathbb{R}$, then using Principle 3.2, the location of the element $u(2, 2) - u(1, 2)$ is at the point $(\frac{1}{2}(2+1), \frac{1}{2}(2+2)) = (\frac{3}{2}, 2)$.

Moreover, assume $v : A_{\leftrightarrow} \rightarrow \mathbb{R}$, then using Principle 3.3, the location of $\frac{1}{4} \left(v(1, \frac{3}{2}) + v(1, \frac{5}{2}) + v(2, \frac{3}{2}) + v(2, \frac{5}{2}) \right)$ is at the point $(\frac{1}{4}(1+1+2+2), \frac{1}{4}(\frac{3}{2} + \frac{5}{2} + \frac{3}{2} + \frac{5}{2})) = (\frac{3}{2}, 2)$ (see Figure 2).

3.2.2. Grid domains and boundary conditions of the partial difference operators

In the following, elementary difference operators are defined over some images with special grid domains and special boundary conditions. The properties of the images obtained from such difference operators containing their domains and boundary conditions are expressed. These images and their domains are employed to define the new discrete TGV in the upcoming subsections.

Definition 3.5. The first- and second-order gradient operators used for the new discretization are defined as follows:

$$1. \mathcal{D}^{new} = (\mathcal{D}_{x_{\bullet}}^{new}, \mathcal{D}_{y_{\bullet}}^{new}) : \mathcal{U}_{\bullet} \rightarrow \mathcal{U}_{\leftrightarrow} \times \mathcal{U}_{\uparrow},$$

$$(\mathcal{D}^{new} u)_1(n_1, n_2) = \mathcal{D}_{x_{\bullet}}^{new} u(n_1, n_2) = \begin{cases} u(n_1 + \frac{1}{2}, n_2) - u(n_1 - \frac{1}{2}, n_2), & \frac{3}{2} \leq n_1 \leq N_1 - \frac{1}{2}, 1 \leq n_2 \leq N_2, \\ 0, & \text{else,} \end{cases} \quad (23)$$

$$(\mathcal{D}^{new}u)_2(n_1, n_2) = \mathcal{D}_{y\bullet}^{new}u(n_1, n_2) = \begin{cases} u(n_1, n_2 + \frac{1}{2}) - u(n_1, n_2 - \frac{1}{2}), & 1 \leq n_1 \leq N_1, \frac{3}{2} \leq n_2 \leq N_2 - \frac{1}{2}, \\ 0, & \text{else,} \end{cases} \quad (24)$$

$$2. \mathcal{E}^{new} = \begin{pmatrix} \mathcal{D}_{x\leftrightarrow}^{new} & 0 \\ 0 & \mathcal{D}_{y\updownarrow}^{new} \\ \frac{1}{2}\mathcal{D}_{y\leftrightarrow}^{new} & \frac{1}{2}\mathcal{D}_{x\updownarrow}^{new} \end{pmatrix} : \mathcal{U}_{\leftrightarrow} \times \mathcal{U}_{\updownarrow} \rightarrow \bar{\mathcal{U}}_{\bullet}^x \times \bar{\mathcal{U}}_{\bullet}^y \times \mathcal{U}_{\times},$$

$$(\mathcal{E}^{new}v)_1(n_1, n_2) = \mathcal{D}_{x\leftrightarrow}^{new}v_1(n_1, n_2) = \begin{cases} v_1(n_1 + \frac{1}{2}, n_2) - v_1(n_1 - \frac{1}{2}, n_2), & 1 \leq n_1 \leq N_1, 1 \leq n_2 \leq N_2, \\ 0, & \text{else,} \end{cases} \quad (25)$$

$$(\mathcal{E}^{new}v)_2(n_1, n_2) = \mathcal{D}_{y\updownarrow}^{new}v_2(n_1, n_2) = \begin{cases} v_2(n_1, n_2 + \frac{1}{2}) - v_2(n_1, n_2 - \frac{1}{2}), & 1 \leq n_1 \leq N_1, 1 \leq n_2 \leq N_2, \\ 0, & \text{else,} \end{cases} \quad (26)$$

$$(\mathcal{E}^{new}v)_3 = \frac{1}{2}(\mathcal{D}_{y\leftrightarrow}^{new}v_1 + \mathcal{D}_{x\updownarrow}^{new}v_2), \text{ where}$$

$$\mathcal{D}_{x\updownarrow}^{new}v_2(n_1, n_2) = \begin{cases} v_2(n_1 + \frac{1}{2}, n_2) - v_2(n_1 - \frac{1}{2}, n_2), & \frac{3}{2} \leq n_1 \leq N_1 - \frac{1}{2}, \frac{1}{2} \leq n_2 \leq N_2 + \frac{1}{2}, \\ 0, & \text{else,} \end{cases} \quad (27)$$

and

$$\mathcal{D}_{y\leftrightarrow}^{new}v_1(n_1, n_2) = \begin{cases} v_1(n_1, n_2 + \frac{1}{2}) - v_1(n_1, n_2 - \frac{1}{2}), & \frac{1}{2} \leq n_1 \leq N_1 + \frac{1}{2}, \frac{3}{2} \leq n_2 \leq N_2 - \frac{1}{2}, \\ 0, & \text{else.} \end{cases} \quad (28)$$

$$3. \mathcal{D}^{2new} : \mathcal{U}_{\bullet} \rightarrow \bar{\mathcal{U}}_{\bullet}^x \times \bar{\mathcal{U}}_{\bullet}^y \times \mathcal{U}_{\times}, \mathcal{D}^{2new}u = \mathcal{E}^{new}\mathcal{D}^{new}u.$$

3.3. Divergences; grid domains, and boundary conditions

In the sequel, we need the dual of operators in Definition 3.5. By requiring a discrete Gauss–Green theorem, the dual operators are obtained as follows:

$$1. \operatorname{div}^{new} = -(\mathcal{D}^{new})^* : \mathcal{U}_{\leftrightarrow} \times \mathcal{U}_{\updownarrow} \rightarrow \mathcal{U}_{\bullet}, \operatorname{div}^{new}(v_1, v_2) = -\mathcal{D}_{x\leftrightarrow}^{new}v_1 - \mathcal{D}_{y\updownarrow}^{new}v_2, \text{ where}$$

$$\mathcal{D}_{x\leftrightarrow}^{new}v_1(n_1, n_2) = \begin{cases} v_1(\frac{3}{2}, n_2), & n_1 = 1, 1 \leq n_2 \leq N_2, \\ v_1(n_1 + \frac{1}{2}, n_2) - v_1(n_1 - \frac{1}{2}, n_2), & 2 \leq n_1 \leq N_1 - 1, 1 \leq n_2 \leq N_2, \\ -v_1(N_1 - \frac{1}{2}, n_2), & n_1 = N_1, 1 \leq n_2 \leq N_2, \end{cases} \quad (29)$$

$$\mathcal{D}_{y\updownarrow}^{new}v_2(n_1, n_2) = \begin{cases} v_2(n_1, \frac{3}{2}), & 1 \leq n_1 \leq N_1, n_2 = 1, \\ v_2(n_1, n_2 + \frac{1}{2}) - v_2(n_1, n_2 - \frac{1}{2}), & 1 \leq n_1 \leq N_1, 2 \leq n_2 \leq N_2 - 1, \\ -v_2(n_1, N_2 - \frac{1}{2}), & 1 \leq n_1 \leq N_1, n_2 = N_2. \end{cases} \quad (30)$$

Note that although $\mathcal{D}_{x\leftrightarrow}^{new}$ and $\mathcal{D}_{y\updownarrow}^{new}$ share the same notation as the operators defined in (25) and (26), their domains of definition differ. In the following we ensure that the latter are always clear from the context such that there is no chance of confusion.

$$2. \operatorname{div}^{new} = -(\mathcal{E}^{new})^* : \bar{\mathcal{U}}_{\bullet}^x \times \bar{\mathcal{U}}_{\bullet}^y \times \mathcal{U}_{\times} \rightarrow \mathcal{U}_{\leftrightarrow} \times \mathcal{U}_{\updownarrow}, \operatorname{div}^{new}v = \begin{pmatrix} \mathcal{D}_{x\bullet}^{new}v_1 + \mathcal{D}_{y\times}^{new}v_3 \\ \mathcal{D}_{y\bullet}^{new}v_2 + \mathcal{D}_{x\times}^{new}v_3 \end{pmatrix}, \text{ where } \mathcal{D}_{x\bullet}^{new} : \bar{\mathcal{U}}_{\bullet}^x \rightarrow \mathcal{U}_{\leftrightarrow}$$

and $\mathcal{D}_{y\bullet}^{new} : \bar{\mathcal{U}}_{\bullet}^y \rightarrow \mathcal{U}_{\updownarrow}$ are defined by

$$\mathcal{D}_{x\bullet}^{new}v_1(n_1, n_2) = \begin{cases} -v_1(1, n_2), & n_1 = \frac{1}{2}, 1 \leq n_2 \leq N_2, \\ v_1(n_1 + \frac{1}{2}, n_2) - v_1(n_1 - \frac{1}{2}, n_2), & \frac{3}{2} \leq n_1 \leq N_1 - \frac{1}{2}, 1 \leq n_2 \leq N_2, \\ v_1(N_1, n_2), & n_1 = N_1 + \frac{1}{2}, 1 \leq n_2 \leq N_2, \end{cases} \quad (31)$$

$$\mathcal{D}_{y\bullet}^{new}v_2(n_1, n_2) = \begin{cases} -v_2(n_1, 1), & 1 \leq n_1 \leq N_1, n_2 = \frac{1}{2}, \\ v_2(n_1, n_2 + \frac{1}{2}) - v_2(n_1, n_2 - \frac{1}{2}), & 1 \leq n_1 \leq N_1, \frac{3}{2} \leq n_2 \leq N_2 - \frac{1}{2}, \\ v_2(n_1, N_2), & 1 \leq n_1 \leq N_1, n_2 = N_2 + \frac{1}{2}. \end{cases} \quad (32)$$

and

$$\mathcal{D}_{x\times}^{new}v_3(n_1, n_2) = \begin{cases} v_3(\frac{3}{2}, n_2), & n_1 = 1, \frac{1}{2} \leq n_2 \leq N_2 + \frac{1}{2}, \\ v_3(n_1 + \frac{1}{2}, n_2) - v_3(n_1 - \frac{1}{2}, n_2), & 2 \leq n_1 \leq N_1 - 1, \frac{1}{2} \leq n_2 \leq N_2 + \frac{1}{2}, \\ -v_3(N_1 - \frac{1}{2}, n_2), & n_1 = N_1, \frac{1}{2} \leq n_2 \leq N_2 + \frac{1}{2}, \end{cases} \quad (33)$$

$$\mathcal{D}_{y \times}^{new} v_3(n_1, n_2) = \begin{cases} v_3(n_1, \frac{3}{2}), & \frac{1}{2} \leq n_1 \leq N_1 + \frac{1}{2}, n_2 = 1, \\ v_3(n_1, n_2 + \frac{1}{2}) - v_3(n_1, n_2 - \frac{1}{2}), & \frac{1}{2} \leq n_1 \leq N_1 + \frac{1}{2}, 2 \leq n_2 \leq N_2 - 1, \\ -v_3(n_1, N_2 - \frac{1}{2}), & \frac{1}{2} \leq n_1 \leq N_1 + \frac{1}{2}, n_2 = N_2, \end{cases} \quad (34)$$

As above, it will be clear from the context which of the definitions of div^{new} is meant.

$$3. \text{div}^{2new} = (\mathcal{D}^{2new}) : \bar{\mathcal{U}}_\bullet^x \times \bar{\mathcal{U}}_\bullet^y \times \mathcal{U}_\times \rightarrow \mathcal{U}_\bullet, \text{div}^{2new} v = \text{div}^{new} \text{div}^{new} v.$$

Indeed, one can verify that with the above definitions, a discrete Gauss–Green theorem as follows holds for $u \in \mathcal{U}_\bullet$ and $v \in \bar{\mathcal{U}}_\bullet^x \times \bar{\mathcal{U}}_\bullet^y \times \mathcal{U}_\times$:

$$\langle u, \text{div}^{2new} v \rangle = -\langle \mathcal{D}^{new} u, \text{div}^{new} v \rangle = \langle \mathcal{D}^{2new} u, v \rangle. \quad (35)$$

3.4. Grid interpolation

3.4.1. Conversion operators

Assume $w = \begin{pmatrix} w_1 \\ w_2 \end{pmatrix} \in \mathcal{U}_\leftrightarrow \times \mathcal{U}_\uparrow$ and $v = (v_1, v_2, v_3)^T \in \bar{\mathcal{U}}_\bullet^x \times \bar{\mathcal{U}}_\bullet^y \times \mathcal{U}_\times$. We define linear grid domain conversion operators $L_\bullet : \mathcal{U}_\leftrightarrow \times \mathcal{U}_\uparrow \rightarrow \mathcal{U}_\bullet \times \mathcal{U}_\bullet$, $L_\leftrightarrow : \mathcal{U}_\leftrightarrow \times \mathcal{U}_\uparrow \rightarrow \mathcal{U}_\leftrightarrow \times \mathcal{U}_\leftrightarrow$ and $L_\uparrow : \mathcal{U}_\leftrightarrow \times \mathcal{U}_\uparrow \rightarrow \mathcal{U}_\uparrow \times \mathcal{U}_\uparrow$ as follows:

$$\begin{aligned} (L_\bullet w)_1(n_1, n_2) &= \frac{1}{2}(w_1(n_1 + \frac{1}{2}, n_2) + w_1(n_1 - \frac{1}{2}, n_2)), & 1 \leq n_1 \leq N_1, 1 \leq n_2 \leq N_2, \\ (L_\bullet w)_2(n_1, n_2) &= \frac{1}{2}(w_2(n_1, n_2 + \frac{1}{2}) + w_2(n_1, n_2 - \frac{1}{2})), & 1 \leq n_1 \leq N_1, 1 \leq n_2 \leq N_2, \\ (L_\leftrightarrow w)_1(n_1, n_2) &= w_1(n_1, n_2), & \frac{1}{2} \leq n_1 \leq N_1 + \frac{1}{2}, 1 \leq n_2 \leq N_2, \\ (L_\leftrightarrow w)_2(n_1, n_2) &= \begin{cases} \frac{1}{4}(w_2(1, n_2 - \frac{1}{2}) + w_2(1, n_2 + \frac{1}{2})), & n_1 = \frac{1}{2}, 1 \leq n_2 \leq N_2, \\ \frac{1}{4}(w_2(n_1 - \frac{1}{2}, n_2 - \frac{1}{2}) + w_2(n_1 - \frac{1}{2}, n_2 + \frac{1}{2}) \\ \quad + w_2(n_1 + \frac{1}{2}, n_2 - \frac{1}{2}) + w_2(n_1 + \frac{1}{2}, n_2 + \frac{1}{2})), & \frac{3}{2} \leq n_1 \leq N_2 - \frac{1}{2}, 1 \leq n_2 \leq N_2, \\ \frac{1}{4}(w_2(N_1, n_2 - \frac{1}{2}) + w_2(N_1, n_2 + \frac{1}{2})), & n_1 = N_1 + \frac{1}{2}, 1 \leq n_2 \leq N_2, \end{cases} \\ (L_\uparrow w)_1(n_1, n_2) &= \begin{cases} \frac{1}{4}(w_1(n_1 - \frac{1}{2}, 1) + w_1(n_1 + \frac{1}{2}, 1)), & 1 \leq n_1 \leq N_1, n_2 = \frac{1}{2}, \\ \frac{1}{4}(w_1(n_1 - \frac{1}{2}, n_2 - \frac{1}{2}) + w_1(n_1 - \frac{1}{2}, n_2 + \frac{1}{2}) \\ \quad + w_1(n_1 + \frac{1}{2}, n_2 - \frac{1}{2}) + w_1(n_1 + \frac{1}{2}, n_2 + \frac{1}{2})), & 1 \leq n_1 \leq N_1, \frac{3}{2} \leq n_2 \leq N_2 - \frac{1}{2}, \\ \frac{1}{4}(w_1(n_1 - \frac{1}{2}, N_2) + w_1(n_1 + \frac{1}{2}, N_2)), & 1 \leq n_1 \leq N_1, n_2 = N_2 + \frac{1}{2}, \end{cases} \\ (L_\uparrow w)_2(n_1, n_2) &= w_2(n_1, n_2), & 1 \leq n_1 \leq N_1, \frac{1}{2} \leq n_2 \leq N_2 + \frac{1}{2}. \end{aligned} \quad (36)$$

Note that at some points in the above definitions, we extended the respective grid in a natural manner and assumed zero values in order to adhere to Principle 3.3. Moreover, the linear operator $L_\bullet : \bar{\mathcal{U}}_\bullet^x \times \bar{\mathcal{U}}_\bullet^y \times \mathcal{U}_\times \rightarrow \mathcal{U}_\bullet \times \mathcal{U}_\bullet \times \mathcal{U}_\bullet$ is defined by

$$\begin{aligned} (L_\bullet v)_1(n_1, n_2) &= v_1(n_1, n_2), & 1 \leq n_1 \leq N_1, 1 \leq n_2 \leq N_2, \\ (L_\bullet v)_2(n_1, n_2) &= v_2(n_1, n_2), & 1 \leq n_1 \leq N_1, 1 \leq n_2 \leq N_2, \\ (L_\bullet v)_3(n_1, n_2) &= \frac{1}{4}(v_3(n_1 - \frac{1}{2}, n_2 - \frac{1}{2}) + v_3(n_1 - \frac{1}{2}, n_2 + \frac{1}{2}) + v_3(n_1 + \frac{1}{2}, n_2 - \frac{1}{2}) + v_3(n_1 + \frac{1}{2}, n_2 + \frac{1}{2})), \\ & & 1 \leq n_1 \leq N_1, 1 \leq n_2 \leq N_2. \end{aligned} \quad (37)$$

Again, in the sequel, the domain of L_\bullet is made clear such that this operator cannot be confused with the previously-defined operator with the same notation. In summary, L_\bullet are operators that convert the grid domain of each component of a given image to an image on A_\bullet , L_\leftrightarrow is a similar grid domain conversion operator to A_\leftrightarrow and L_\uparrow is a similar grid domain conversion operator to A_\uparrow .

3.5. Proposed model and its Fenchel–Rockafellar dual

3.5.1. Formulation of the discrete TGV functional

Now, we propose the following discretization of TGV of order 2 according to (4):

$$\begin{aligned} \text{TGV}_\alpha^{2(new)}(u) &= \max_{v, w} \left\{ \langle u, s \rangle : v \in \bar{\mathcal{U}}_\bullet^x \times \bar{\mathcal{U}}_\bullet^y \times \mathcal{U}_\bullet, w \in \mathcal{U}_\leftrightarrow \times \mathcal{U}_\uparrow, \|L_\bullet v\|_\infty \leq \alpha_0, \|L_\bullet w\|_\infty \leq \alpha_1, \right. \\ & \quad \left. \|L_\leftrightarrow w\|_\infty \leq \alpha_1, \|L_\uparrow w\|_\infty \leq \alpha_1, w = \text{div}^{new} v, s = \text{div}^{new} w \right\}, \end{aligned} \quad (38)$$

where

$$\begin{aligned} \|L_\star w\|_\infty &= \max\{\sqrt{(L_\star w)_1(n_1, n_2)^2 + (L_\star w)_2(n_1, n_2)^2} : (n_1, n_2) \in A_\star\}, \star = \bullet, \leftrightarrow, \updownarrow, \\ \|L_\bullet v\|_\infty &= \max\{\sqrt{(L_\bullet v)_1(n_1, n_2)^2 + (L_\bullet v)_2(n_1, n_2)^2 + 2(L_\bullet v)_3(n_1, n_2)^2} : (n_1, n_2) \in A_\bullet\}. \end{aligned} \quad (39)$$

In the formulation of classic discrete TGV (22), two constraints are used; $\|v\|_\infty \leq \alpha_0$ and $\|\operatorname{div} v\|_\infty \leq \alpha_1$, whereas in the new proposed discrete TGV (38), we use four constraints; $\|L_\bullet v\|_\infty \leq \alpha_0$, $\|L_\bullet(\operatorname{div}^{new} v)\|_\infty \leq \alpha_1$, $\|L_{\leftrightarrow}(\operatorname{div}^{new} v)\|_\infty \leq \alpha_1$ and $\|L_{\updownarrow}(\operatorname{div}^{new} v)\|_\infty \leq \alpha_1$. In other words, instead of the boundedness of the vector field v and the tensor field v , we impose boundedness for their converted versions.

Let us revisit the operators div and div^2 of Subsection 2.5 in view of Principles 3.2 and 3.3. Then, $\operatorname{div} : (\mathbb{R}^2)^{N_1 \times N_2} \rightarrow \mathbb{R}^{N_1 \times N_2}$ can be interpreted as $\operatorname{div} : \mathcal{U}_\leftrightarrow \times \mathcal{U}_{\updownarrow} \rightarrow \mathcal{U}_\bullet$ if we identify $\mathcal{U}_\bullet \triangleq \mathbb{R}^{N_1 \times N_2}$, $\mathcal{U}_{\leftrightarrow} \triangleq (\mathbb{R}^{1 \times N_2} + (-\frac{1}{2}, 0)) \times (\mathbb{R}^{N_1 \times N_2} + (\frac{1}{2}, 0))$, $\mathcal{U}_{\updownarrow} \triangleq (\mathbb{R}^{N_1 \times 1} + (0, -\frac{1}{2})) \times (\mathbb{R}^{N_1 \times N_2} + (0, \frac{1}{2}))$, where $+$ denotes an index shift and the entries that do not correspond to $\mathbb{R}^{N_1 \times N_2}$ are filled with zero. Likewise $\operatorname{div} : S(\mathbb{R}^4)^{N_1 \times N_2} \rightarrow (\mathbb{R}^2)^{N_1 \times N_2}$ can be interpreted as $\operatorname{div} : \bar{\mathcal{U}}_\bullet^x \times \bar{\mathcal{U}}_\bullet^y \times \mathcal{U}_\bullet \rightarrow \mathcal{U}_{\leftrightarrow} \times \mathcal{U}_{\updownarrow}$ by the identification $(v_1, v_2, v_3) \triangleq \begin{pmatrix} v_1 & v_3 \\ v_3 & v_2 \end{pmatrix}$ and $\bar{\mathcal{U}}_\bullet^x \triangleq (\mathbb{R}^{1 \times N_2} + (-1, 0)) \times \mathbb{R}^{N_1 \times N_2} \times (\mathbb{R}^{1 \times N_2} + (N_1, 0))$, $\bar{\mathcal{U}}_\bullet^y \triangleq (\mathbb{R}^{N_1 \times 1} + (0, -1)) \times \mathbb{R}^{N_1 \times N_2} \times (\mathbb{R}^{N_1 \times 1} + (0, N_2))$, $\mathcal{U}_\times \triangleq (\mathbb{R}^{N_1 \times N_2} \times (\mathbb{R}^{1 \times (N_2+1)} + (-\frac{1}{2}, -\frac{1}{2})) \times (\mathbb{R}^{N_1 \times 1} + (\frac{1}{2}, -\frac{1}{2})) \times (\mathbb{R}^{N_1 \times N_2} + (\frac{1}{2}, \frac{1}{2}))$, where again $+$ denotes an index shift and the entries that do not correspond to $\mathbb{R}^{N_1 \times N_2}$ are filled with zero. With the index shifts introduced in the above identifications, the constraints in the classic discrete second-order TGV according to (22) correspond to:

$$\sqrt{v_1(n_1, n_2)^2 + v_2(n_1, n_2)^2 + 2v_3(n_1 + \frac{1}{2}, n_2 + \frac{1}{2})^2} \leq \alpha_0, \quad \sqrt{(\operatorname{div} v)_1(n_1 + \frac{1}{2}, n_2)^2 + (\operatorname{div} v)_2(n_1, n_2 + \frac{1}{2})^2} \leq \alpha_1, \quad (40)$$

for $v \in \bar{\mathcal{U}}_\bullet^x \times \bar{\mathcal{U}}_\bullet^y \times \mathcal{U}_\bullet$ and $(n_1, n_2) \in A_\bullet$. The constraint in the left hand-side of (40) is the square root of the addition of two elements on the common grid A_\bullet (subset of both \bar{A}_\bullet^x and \bar{A}_\bullet^y), whereas the third element corresponds to the shifted grid A_\times . Likewise, in the right-hand side constraint, two elements of the different grids A_{\leftrightarrow} and A_{\updownarrow} are added. In other words, for both constraints, there exists an inconsistency in terms of the grid point evaluation.

As it is explained before, if $u \in \mathcal{U}_\bullet$, then $\mathcal{D}^{new} u, \operatorname{div}^{new} v \in \mathcal{U}_\leftrightarrow \times \mathcal{U}_{\updownarrow}$, $\mathcal{D}^2 u, v \in \bar{\mathcal{U}}_\bullet^x \times \bar{\mathcal{U}}_\bullet^y \times \mathcal{U}_\times$. Assume $w_1 = (\operatorname{div}^{new} v)_1$, $w_2 = (\operatorname{div}^{new} v)_2$, then the constraints in optimization problem (38) can be expressed by

$$\begin{aligned} \sqrt{(L_\star w)_1(n_1, n_2)^2 + (L_\star w)_2(n_1, n_2)^2} &\leq \alpha_1, (n_1, n_2) \in A_\star, \star = \bullet, \leftrightarrow, \updownarrow, \\ \sqrt{(L_\bullet v)_1(n_1, n_2)^2 + (L_\bullet v)_2(n_1, n_2)^2 + 2(L_\bullet v)_3(n_1, n_2)^2} &\leq \alpha_0, (n_1, n_2) \in A_\bullet, \end{aligned} \quad (41)$$

where $(L_\star w_1), (L_\star w_2) \in A_\star$, $L_\bullet v_1, L_\bullet v_2, L_\bullet v_3 \in A_\bullet$. Therefore, the norm definitions in (41) admit grid domain consistency. Moreover, another difference of the classic discrete TGV in comparison to the new proposed one is the rotationally invariance, with respect to 90° rotation. This property is discussed in the next section.

Remark 3.6. Note that other choices of interpolation operators in (38) are possible. Generally, we can define operators converting elements of $v \in \bar{\mathcal{U}}_\bullet^x \times \bar{\mathcal{U}}_\bullet^y \times \mathcal{U}_\bullet$ and $w \in \mathcal{U}_{\leftrightarrow} \times \mathcal{U}_{\updownarrow}$ to respective versions on the grids $A_\bullet, A_{\leftrightarrow}, A_{\updownarrow}, A_\times$, resulting in 8 operators, denoted by $L_\bullet, L_{\leftrightarrow}, L_{\updownarrow}, L_\times$ with a slight abuse of notation. In principle, any non-empty subset of these operators applied to v and w would also be possible in (38). As it can be observed, (38) only contains the operator L_\bullet for v and the three conversion operators $L_{\leftrightarrow}, L_{\updownarrow}$ and L_\bullet for w . As v contains two components in the extended center grids $\bar{A}_\bullet^x, \bar{A}_\bullet^y$ which are supersets of A_\bullet , and one component in corner grid A_\times , we preferred to use only the conversion operator L_\bullet . For the variable w , as the components belong to $\mathcal{U}_{\leftrightarrow}$ and $\mathcal{U}_{\updownarrow}$, we use the conversion operators L_{\leftrightarrow} and L_{\updownarrow} as well as the natural conversion operator L_\bullet . This selection realizes a good trade-off between accuracy and efficiency. Also, as we will see in Section 4, the choice of conversion operators allow us to prove a 90° rotational invariance property. In contrast, the classic discrete TGV is not invariant with respect to 90° rotations.

3.5.2. Fenchel-Rockafellar dual of the proposed model

In this subsection we find a dual form for the proposed new discrete TGV (38). We need such formulation to employ a primal-dual algorithm to solve corresponding denoising and inverse problems. Define

$$\begin{aligned} K &= \{(v, w, s) \in (\bar{\mathcal{U}}_\bullet^x \times \bar{\mathcal{U}}_\bullet^y \times \mathcal{U}_\bullet) \times (\mathcal{U}_{\leftrightarrow} \times \mathcal{U}_{\updownarrow}) \times \mathcal{U}_\bullet : |L_\bullet v(n_1, n_2)| \leq \alpha_0 \ \forall (n_1, n_2) \in A_\bullet, \\ &\quad |L_\star w(n_1, n_2)| \leq \alpha_1, \star = \bullet, \leftrightarrow, \updownarrow \ \forall (n_1, n_2) \in A_\star, w = -\operatorname{div}^{new} v, s = -\operatorname{div}^{new} w\}. \end{aligned} \quad (42)$$

Then, obviously

$$\text{TGV}_\alpha^{2(\text{new})}(u) = \max_{(v,w,s)} \langle u, s \rangle - I_K(v, w, s), \quad (43)$$

where $I_K(t) = \begin{cases} 0, & t \in K \\ \infty, & t \notin K \end{cases}$. We aim at finding a dual definition of $\text{TGV}_\alpha^{2(\text{new})}$. For this purpose, the adjoint operators of L_\bullet , L_\leftrightarrow and L_\uparrow are calculated in the following.

Let $w_\bullet = \begin{pmatrix} w_\bullet^1 \\ w_\bullet^2 \end{pmatrix} \in \mathcal{U}_\bullet \times \mathcal{U}_\bullet$, $w_\leftrightarrow = \begin{pmatrix} w_\leftrightarrow^1 \\ w_\leftrightarrow^2 \end{pmatrix} \in \mathcal{U}_\leftrightarrow \times \mathcal{U}_\leftrightarrow$, $w_\uparrow = \begin{pmatrix} w_\uparrow^1 \\ w_\uparrow^2 \end{pmatrix} \in \mathcal{U}_\uparrow \times \mathcal{U}_\uparrow$. Then, we have the following adjoint operators $L_\bullet^* : \mathcal{U}_\bullet \times \mathcal{U}_\bullet \rightarrow \mathcal{U}_\leftrightarrow \times \mathcal{U}_\uparrow$, $L_\leftrightarrow^* : \mathcal{U}_\leftrightarrow \times \mathcal{U}_\leftrightarrow \rightarrow \mathcal{U}_\leftrightarrow \times \mathcal{U}_\uparrow$ and $L_\uparrow^* : \mathcal{U}_\uparrow \times \mathcal{U}_\uparrow \rightarrow \mathcal{U}_\leftrightarrow \times \mathcal{U}_\uparrow$:

$$\begin{aligned} (L_\bullet^* w_\bullet)_1(n_1, n_2) &= \begin{cases} \frac{1}{2} w_\bullet^1(1, n_2), & n_1 = \frac{1}{2}, 1 \leq n_2 \leq N_2, \\ \frac{1}{2} (w_\bullet^1(n_1 + \frac{1}{2}, n_2) + w_\bullet^1(n_1 - \frac{1}{2}, n_2)), & \frac{3}{2} \leq n_1 \leq N_1 - \frac{1}{2}, 1 \leq n_2 \leq N_2, \\ \frac{1}{2} w_\bullet^1(N_1, n_2), & n_1 = N_1 + \frac{1}{2}, 1 \leq n_2 \leq N_2, \\ \frac{1}{2} w_\bullet^2(n_1, 1), & 1 \leq n_1 \leq N_1, n_2 = \frac{1}{2}, \\ \frac{1}{2} (w_\bullet^2(n_1, n_2 + \frac{1}{2}) + w_\bullet^2(n_1, n_2 - \frac{1}{2})), & 1 \leq n_1 \leq N_1, \frac{3}{2} \leq n_2 \leq N_2 - \frac{1}{2}, \\ \frac{1}{2} w_\bullet^2(n_1, N_2), & 1 \leq n_1 \leq N_1, n_2 = N_2 + \frac{1}{2}. \end{cases} \\ (L_\bullet^* w_\bullet)_2(n_1, n_2) &= \begin{cases} w_\leftrightarrow^1(n_1, n_2), & \frac{1}{2} \leq n_1 \leq N_1 + \frac{1}{2}, 1 \leq n_2 \leq N_2, \\ \frac{1}{4} (w_\leftrightarrow^2(n_1 + \frac{1}{2}, 1) + w_\leftrightarrow^2(n_1 - \frac{1}{2}, 1)), & 1 \leq n_1 \leq N_1, n_2 = \frac{1}{2}, \\ \frac{1}{4} (w_\leftrightarrow^2(n_1 + \frac{1}{2}, n_2 - \frac{1}{2}) + w_\leftrightarrow^2(n_1 - \frac{1}{2}, n_2 - \frac{1}{2}) \\ \quad + w_\leftrightarrow^2(n_1 + \frac{1}{2}, n_2 + \frac{1}{2}) + w_\leftrightarrow^2(n_1 - \frac{1}{2}, n_2 + \frac{1}{2})), & 1 \leq n_1 \leq N_1, \frac{3}{2} \leq n_2 \leq N_2 - \frac{1}{2}, \\ \frac{1}{4} (w_\leftrightarrow^2(n_1 + \frac{1}{2}, N_2) + w_\leftrightarrow^2(n_1 - \frac{1}{2}, N_2)), & 1 \leq n_1 \leq N_1, n_2 = N_2 + \frac{1}{2}, \end{cases} \\ (L_\uparrow^* w_\uparrow)_1(n_1, n_2) &= \begin{cases} \frac{1}{4} (w_\uparrow^1(1, n_2 - \frac{1}{2}) + w_\uparrow^1(1, n_2 + \frac{1}{2})), & n_1 = \frac{1}{2}, 1 \leq n_2 \leq N_2, \\ \frac{1}{4} (w_\uparrow^1(n_1 + \frac{1}{2}, n_2 - \frac{1}{2}) + w_\uparrow^1(n_1 - \frac{1}{2}, n_2 - \frac{1}{2}) \\ \quad + w_\uparrow^1(n_1 + \frac{1}{2}, n_2 + \frac{1}{2}) + w_\uparrow^1(n_1 - \frac{1}{2}, n_2 + \frac{1}{2})), & \frac{3}{2} \leq n_1 \leq N_1 - \frac{1}{2}, 1 \leq n_2 \leq N_2, \\ \frac{1}{4} (w_\uparrow^1(N_1, n_2 - \frac{1}{2}) + w_\uparrow^1(N_1, n_2 + \frac{1}{2})), & n_1 = N_1 + \frac{1}{2}, 1 \leq n_2 \leq N_2. \end{cases} \\ (L_\uparrow^* w_\uparrow)_2(n_1, n_2) &= w_\uparrow^2(n_1, n_2), \quad 1 \leq n_1 \leq N_1, \frac{1}{2} \leq n_2 \leq N_2 + \frac{1}{2}. \end{aligned} \quad (44)$$

Moreover, for $v_\bullet = \begin{pmatrix} v_\bullet^1 \\ v_\bullet^2 \\ v_\bullet^3 \end{pmatrix} \in \mathcal{U}_\bullet \times \mathcal{U}_\bullet \times \mathcal{U}_\bullet$, the adjoint operator $L_\bullet^* : \mathcal{U}_\bullet \times \mathcal{U}_\bullet \times \mathcal{U}_\bullet \rightarrow \bar{\mathcal{U}}_\bullet^x \times \bar{\mathcal{U}}_\bullet^y \times \mathcal{U}_\times$ reads:

$$\begin{aligned} (L_\bullet^* v_\bullet)_1(n_1, n_2) &= \begin{cases} v_\bullet^1(n_1, n_2), & 1 \leq n_1 \leq N_1, 1 \leq n_2 \leq N_2, \\ 0, & n_1 = 0, N_1 + 1, 1 \leq n_2 \leq N_2, \\ v_\bullet^2(n_1, n_2), & 1 \leq n_1 \leq N_1, 1 \leq n_2 \leq N_2, \\ 0, & 1 \leq n_2 \leq N_2, n_2 = 0, N_2 + 1, \end{cases} \\ (L_\bullet^* v_\bullet)_2(n_1, n_2) &= \begin{cases} \frac{1}{4} v_\bullet^3(1, 1), & n_1 = n_2 = \frac{1}{2}, \\ \frac{1}{4} (v_\bullet^3(1, n_2 - \frac{1}{2}) + v_\bullet^3(1, n_2 + \frac{1}{2})), & n_1 = \frac{1}{2}, \frac{3}{2} \leq n_2 \leq N_2 - \frac{1}{2}, \\ \frac{1}{4} v_\bullet^3(1, N_2), & n_1 = \frac{1}{2}, n_2 = N_2 + \frac{1}{2}, \\ \frac{1}{4} ((v_\bullet^3(n_1 - \frac{1}{2}, 1) + (v_\bullet^3(n_1 + \frac{1}{2}, 1))) \\ \quad + (v_\bullet^3(n_1 - \frac{1}{2}, n_2 - \frac{1}{2}) + (v_\bullet^3(n_1 + \frac{1}{2}, n_2 - \frac{1}{2})) \\ \quad + (v_\bullet^3(n_1 - \frac{1}{2}, n_2 + \frac{1}{2}) + (v_\bullet^3(n_1 + \frac{1}{2}, n_2 + \frac{1}{2}))), & \frac{3}{2} \leq n_1 \leq N_1 - \frac{1}{2}, \frac{3}{2} \leq n_2 \leq N_2 - \frac{1}{2}, \\ \frac{1}{4} (v_\bullet^3(n_1 - \frac{1}{2}, N_2) + v_\bullet^3(n_1 + \frac{1}{2}, N_2)), & \frac{3}{2} \leq n_1 \leq N_1 - \frac{1}{2}, n_2 = N_2 + \frac{1}{2}, \\ \frac{1}{4} v_\bullet^3(N_1, 1), & n_1 = N_1 + \frac{1}{2}, n_2 = \frac{1}{2}, \\ \frac{1}{4} (v_\bullet^3(N_1, n_2 - \frac{1}{2}) + v_\bullet^3(N_1, n_2 + \frac{1}{2})), & n_1 = N_1 + \frac{1}{2}, \frac{3}{2} \leq n_2 \leq N_2 - \frac{1}{2}, \\ \frac{1}{4} v_\bullet^3(N_1, N_2), & n_1 = N_1 + \frac{1}{2}, n_2 = N_2 + \frac{1}{2}. \end{cases} \end{aligned} \quad (45)$$

Now, we define the operator L and the corresponding dual L^* via the following operator matrices:

$$L = \begin{pmatrix} L_\bullet & 0 & 0 \\ 0 & L_\bullet & 0 \\ 0 & L_{\leftrightarrow} & 0 \\ 0 & L_{\updownarrow} & 0 \\ 0 & \text{div}^{new} & I \\ \text{div}^{new} & I & 0 \end{pmatrix}, \quad L^* = \begin{pmatrix} L_\bullet^* & 0 & 0 & 0 & 0 & -\mathcal{E}^{new} \\ 0 & L_\bullet^* & L_{\leftrightarrow}^* & L_{\updownarrow}^* & -\mathcal{D}^{new} & I \\ 0 & 0 & 0 & 0 & I & 0 \end{pmatrix}. \quad (46)$$

In the first column of L , we have $L_\bullet : \bar{\mathcal{U}}_\bullet^x \times \bar{\mathcal{U}}_\bullet^y \times \mathcal{U}_\times \rightarrow \mathcal{U}_\bullet \times \mathcal{U}_\bullet \times \mathcal{U}_\bullet$ while in the second column, $L_\bullet : \mathcal{U}_{\leftrightarrow} \times \mathcal{U}_{\updownarrow} \rightarrow \mathcal{U}_\bullet \times \mathcal{U}_\bullet$. Consequently, in the first row of L^* , we have $L_\bullet^* : \mathcal{U}_\bullet \times \mathcal{U}_\bullet \times \mathcal{U}_\bullet \rightarrow \bar{\mathcal{U}}_\bullet^x \times \bar{\mathcal{U}}_\bullet^y \times \mathcal{U}_\times$ while in the second row, $L_\bullet^* : \mathcal{U}_\bullet \times \mathcal{U}_\bullet \rightarrow \mathcal{U}_{\leftrightarrow} \times \mathcal{U}_{\updownarrow}$. Analogous considerations apply to the operators div^{new} in L .

Remark 3.7. The boundary conditions associated with the adjoint of the above conversion operators are dictated by the adjointness requirement:

$$\langle L_\star^* w_\star, w \rangle = \langle w_\star, L_\star w \rangle, \quad \star = \bullet, \leftrightarrow, \updownarrow, \quad \langle L_\bullet^* v_\bullet, v \rangle = \langle v_\bullet, L_\bullet v \rangle,$$

for each $w \in \mathcal{U}_{\leftrightarrow} \times \mathcal{U}_{\updownarrow}$, $w_\star \in \mathcal{U}_\star \times \mathcal{U}_\star$, $\star = \bullet, \leftrightarrow, \updownarrow$, $v \in \bar{\mathcal{U}}_\bullet^x \times \bar{\mathcal{U}}_\bullet^y \times \mathcal{U}_\times$ and $v_\bullet \in \mathcal{U}_\bullet \times \mathcal{U}_\bullet \times \mathcal{U}_\bullet$.

We employ the following theorem in order to find a dual form of the proposed regularization term [30].

Theorem 3.8. (*Fenchel Duality Theorem*): Assume X, Y are real Banach spaces, $f : X \rightarrow]-\infty, +\infty]$ and $g : Y \rightarrow]-\infty, +\infty]$ are proper, convex and lower-semicontinuous functions and $A : X \rightarrow Y$ is a linear continuous operator, if there exists $x_0 \in X$ such that $f(x_0) < \infty$ and g is continuous at Ax_0 , then

$$\sup_{x \in X} -f(x) - g(Ax) = \min_{y^* \in Y^*} g^*(y^*) + f^*(-A^* y^*), \quad (47)$$

where f^* and g^* are the Fenchel conjugates of f and g , respectively.

Theorem 3.9. The functional $\text{TGV}_\alpha^{2(new)}$ according to (38) satisfies:

$$\begin{aligned} \text{TGV}_\alpha^{2(new)}(u) &= \min_{v_\bullet, w_\bullet, w_{\leftrightarrow}, w_{\updownarrow}, \omega} \alpha_0 \|v_\bullet\|_1 + \alpha_1 \|w_\bullet\|_1 + \alpha_1 \|w_{\leftrightarrow}\|_1 + \alpha_1 \|w_{\updownarrow}\|_1 \\ \text{subject to } &\begin{cases} \mathcal{D}^{new} u - \omega = L_\bullet^* v_\bullet + L_{\leftrightarrow}^* w_{\leftrightarrow} + L_{\updownarrow}^* w_{\updownarrow}, \\ \mathcal{E}^{new} = L_\bullet^* w_\bullet, \end{cases} \end{aligned} \quad (48)$$

where $v_\bullet \in \mathcal{U}_\bullet \times \mathcal{U}_\bullet \times \mathcal{U}_\bullet$, $w_\star \in \mathcal{U}_\star \times \mathcal{U}_\star$, $\star = \bullet, \leftrightarrow, \updownarrow$ and $\omega \in \mathcal{U}_{\leftrightarrow} \times \mathcal{U}_{\updownarrow}$.

Proof. Consider the optimization problem (43). To find the Fenchel dual problem via the Fenchel duality theorem, we define, for a given $u \in \mathcal{U}_\bullet$, $f(v, w, s) = -\langle u, s \rangle$ for $(v, w, s) \in (\bar{\mathcal{U}}_\bullet^x \times \bar{\mathcal{U}}_\bullet^y \times \mathcal{U}_\times) \times (\mathcal{U}_{\leftrightarrow} \times \mathcal{U}_{\updownarrow}) \times \mathcal{U}_\bullet$, $g = I_{\bar{K}}$ where

$$\begin{aligned} \bar{K} = \{ (v_\bullet, w_\bullet, w_{\leftrightarrow}, w_{\updownarrow}, \bar{u}, \omega) \in \mathcal{U}_\bullet^3 \times \mathcal{U}_\bullet^2 \times \mathcal{U}_{\leftrightarrow}^2 \times \mathcal{U}_{\updownarrow}^2 \times \mathcal{U}_\bullet \times (\mathcal{U}_{\leftrightarrow} \times \mathcal{U}_{\updownarrow}) : |v_\bullet(n_1, n_2)| \leq \alpha_0 \ \forall (n_1, n_2) \in A_\bullet, \\ |w_\star(n_1, n_2)| \leq \alpha_1, \star = \bullet, \leftrightarrow, \updownarrow \ \forall (n_1, n_2) \in A_\star, \bar{u} = 0, \omega = 0 \}, \end{aligned} \quad (49)$$

and $A = L$ is defined in (46). Obviously, \bar{K} is non-empty, convex and closed, and therefore, g is proper, convex and lower-semicontinuous. Furthermore, f is convex and continuous. Thus, the assumptions of the Fenchel duality theorem hold.

Now, the optimization problem corresponding to the left hand-side of (47) corresponds to $\text{TGV}_\alpha^{2(new)}(u)$. To find the right hand-side, i.e., the dual minimization problem, the Fenchel conjugates f^*, g^* are needed, whereas the adjoint operator $A^* = L^*$ is already given in (46). Thus, consider

$$f(v, w, s) = -\langle u, s \rangle = \sup_{v^*, w^*, s^*} \langle (v, w, s), (v^*, w^*, s^*) \rangle - I_{\{(0,0,-u)\}}(v^*, w^*, s^*),$$

therefore, $f^*(v, w, s) = I_{\{(0,0,-u)\}}(v, w, s)$. Since the 1-norm is the dual of the ∞ -norm, we get:

$$g^*(v_\bullet, w_\bullet, w_{\leftrightarrow}, w_{\updownarrow}, \bar{u}, \omega) = \alpha_0 \|v_\bullet\|_1 + \alpha_1 \|w_\bullet\|_1 + \alpha_1 \|w_{\leftrightarrow}\|_1 + \alpha_1 \|w_{\updownarrow}\|_1,$$

where

$$\begin{aligned} \|w_\star\|_1 &= \sum_{(n_1, n_2) \in A_\star} |w_\star(n_1, n_2)|, \quad |w_\star(n_1, n_2)| = \sqrt{\sum_{i=1}^2 w_\star^i(n_1, n_2)^2}, \quad \star = \bullet, \leftrightarrow, \updownarrow, \\ \|v_\bullet\|_1 &= \sum_{(n_1, n_2) \in A_\bullet} |v_\bullet(n_1, n_2)|, \quad |v_\bullet(n_1, n_2)| = \sqrt{v_\bullet^1(n_1, n_2)^2 + v_\bullet^2(n_1, n_2)^2 + 2v_\bullet^3(n_1, n_2)^2}. \end{aligned}$$

From the Fenchel duality theorem, we get:

$$\begin{aligned} \text{TGV}_\alpha^{2(\text{new})}(u) &= \min_{v_\bullet, w_\bullet, w_\leftrightarrow, w_\updownarrow, \bar{u}, \omega} \alpha_0 \|v_\bullet\|_1 + \alpha_1 \|w_\bullet\|_1 + \alpha_1 \|w_\leftrightarrow\|_1 + \alpha_1 \|w_\updownarrow\|_1 \\ &\text{subject to} \quad L^*(v_\bullet, w_\bullet, v_\leftrightarrow, v_\updownarrow, \bar{u}, \omega) = 0, \end{aligned}$$

which is equivalent to

$$\begin{aligned} \text{TGV}_\alpha^{2(\text{new})}(u) &= \min_{v_\bullet, w_\bullet, w_\leftrightarrow, w_\updownarrow, \bar{u}, \omega} \alpha_0 \|v_\bullet\|_1 + \alpha_1 \|w_\bullet\|_1 + \alpha_1 \|w_\leftrightarrow\|_1 + \alpha_1 \|w_\updownarrow\|_1 \\ &\text{subject to} \quad \begin{cases} \mathcal{E}^{\text{new}} \omega = L_\bullet^* v_\bullet, \\ \mathcal{D}^{\text{new}} \bar{u} - \omega = L_\bullet^* v_\bullet + L_\leftrightarrow^* v_\leftrightarrow + L_\updownarrow^* v_\updownarrow, \quad u = \bar{u}, \end{cases} \end{aligned}$$

leading to the desired statement. \square

Remark 3.10. Consider the classic discrete version of TGV in (22):

$$\text{TGV}_\alpha^2(u) = \min_{\omega \in (\mathbb{R}^2)^{N_1 \times N_2}} \alpha_1 \|\mathcal{D}u - \omega\|_1 + \alpha_0 \|\mathcal{E}\omega\|_1 \quad (50)$$

which can be rewritten to

$$\begin{aligned} \text{TGV}_\alpha^2(u) &= \min_{w, \omega \in (\mathbb{R}^2)^{N_1 \times N_2}} \alpha_1 \|w\|_1 + \alpha_0 \|v\|_1 \\ &\text{subject to} \quad \begin{cases} \mathcal{D}u - \omega = w, \\ \mathcal{E}\omega = v. \end{cases} \end{aligned} \quad (51)$$

Compare this to the proposed discrete TGV in (48):

$$\begin{aligned} \text{TGV}_\alpha^{2(\text{new})}(u) &= \min_{v_\bullet, w_\bullet, w_\leftrightarrow, w_\updownarrow, \omega} \alpha_1 (\|w_\updownarrow\|_1 + \|w_\leftrightarrow\|_1 + \|w_\bullet\|_1) + \alpha_0 \|v_\bullet\|_1 \\ &\text{subject to} \quad \begin{cases} \mathcal{D}^{\text{new}} u - \omega = L_\bullet^* w_\bullet + L_\leftrightarrow^* w_\leftrightarrow + L_\updownarrow^* w_\updownarrow, \\ \mathcal{E}^{\text{new}} \omega = L_\bullet^* v_\bullet. \end{cases} \end{aligned} \quad (52)$$

It can be seen that in classic discrete TGV, the aim is the minimization of an energy function containing $\alpha_1 \|w\|_1$ and $\alpha_0 \|v\|_1$, where w and v are discrete gradient fields and symmetric matrix fields, respectively. For the newly defined discrete TGV (52), instead of w , three gradient fields, $w_\bullet, w_\leftrightarrow, w_\updownarrow$, are used and penalized with the sum of their respective 1-norms. Likewise, v in the classic discrete TGV is replaced by v_\bullet in the proposed TGV. Moreover, instead of the constraints $\mathcal{D}u - \omega = w$ and $\mathcal{E}\omega = v$, we have the different constraints

$$\mathcal{D}^{\text{new}} u - \omega = L_\bullet^* w_\bullet + L_\leftrightarrow^* w_\leftrightarrow + L_\updownarrow^* w_\updownarrow \quad \text{and} \quad \mathcal{E}^{\text{new}} \omega = L_\bullet^* v_\bullet. \quad (53)$$

To interpret (53), observe that $\mathcal{D}^{\text{new}} u - \omega$ is decomposed into $w_\bullet, w_\leftrightarrow, w_\updownarrow$ which live on the grids $A_\bullet, A_\leftrightarrow, A_\updownarrow$, respectively, and are interpolated, as a consequence of Principle 3.3, to be compatible with $\mathcal{D}^{\text{new}} u - \omega$ whose components live on the grid A_\leftrightarrow and A_\updownarrow , respectively. Minimizing over the sum of the 1-norms of $w_\bullet, w_\leftrightarrow$ and w_\updownarrow thus asks for an optimal decomposition of $\mathcal{D}^{\text{new}} u - \omega$ into vector fields on different grids in terms of the 1-norm, similar (but not identical) to an infimal convolution. Similarly, $\mathcal{E}^{\text{new}} \omega$ can be interpreted to be converted to the grid A_\bullet by choosing a v_\bullet which is interpolated to be compatible to $\mathcal{E}^{\text{new}} \omega$ and whose 1-norm is also penalized.

Note that it is not possible to rewrite this problem to a simplified version without the variables $w_\star, \star = \bullet, \leftrightarrow, \updownarrow$, whereas for the classic discrete TGV, we can simplify (51) to (50).

4. A basic invariance property

In the following, we prove that the new proposed discrete TGV is 90° rotationally invariant, which can be expected as a consequence of the proposed building blocks. However, as mentioned before, this property is not fulfilled for the classic discrete second-order TGV. For this purpose, denote by A_\bullet^\perp , $A_{\leftrightarrow}^\perp$, A_\uparrow^\perp , $\bar{A}_\bullet^{x\perp}$, $\bar{A}_\bullet^{y\perp}$ and A_\times^\perp the grids according to Definition 3.1 with N_1 and N_2 interchanged. The resulting function spaces will also be marked with a $^\perp$, i.e., $\mathcal{U}_\bullet^\perp$ for the functions on A_\bullet^\perp and so on. Since there will be no chance of confusion, we will use the same notation for the operators on the functions spaces involving original and rotated grids such as \mathcal{D}^{new} , \mathcal{E}^{new} , L_\bullet^* , L_{\leftrightarrow}^* , L_\uparrow^* etc.

Theorem 4.1. (90° isotropy) *Let $u \in \mathcal{U}_\bullet$ and let $\mathcal{R}u \in \mathcal{U}_\bullet^\perp$ be the 90° rotated image, that is, u applied to $\mathcal{R} : \mathcal{U}_\bullet \rightarrow \mathcal{U}_\bullet^\perp$, the 90° rotation operator mapping $u \in \mathcal{U}_\bullet$ to*

$$\mathcal{R}u(n_1, n_2) = u(n_2, N_2 - n_1 + 1), \quad n_1 = 1, 2, \dots, N_2, n_2 = 1, 2, \dots, N_1.$$

Then, $TGV_\alpha^{2(new)}(\mathcal{R}u) = TGV_\alpha^{2(new)}(u)$ where the functional has to be understood in the respective domain.

Proof. First note that the reparametrization $(n_1, n_2) \mapsto (n_2, N_2 + 1 - n_1)$ is a bijection when mapping as follows: $A_\bullet \rightarrow A_\bullet^\perp$, $A_{\leftrightarrow} \rightarrow A_\uparrow^\perp$, $A_\uparrow \rightarrow A_{\leftrightarrow}^\perp$, $\bar{A}_\bullet^x \rightarrow \bar{A}_\bullet^{y\perp}$, $\bar{A}_\bullet^y \rightarrow \bar{A}_\bullet^{x\perp}$ and $A_\times \rightarrow A_\times^\perp$. Consequently, \mathcal{R} considered as a map between $\mathcal{U}_\bullet \rightarrow \mathcal{U}_\bullet^\perp$ is a linear isomorphism. The same applies to the analogous versions, i.e., $\mathcal{R} : \mathcal{U}_{\leftrightarrow} \rightarrow \mathcal{U}_\uparrow^\perp$ etc. With these preparations, we see, for instance, for $u \in \mathcal{U}_\bullet$ that

$$\begin{aligned} (\mathcal{D}_{x_\bullet}^{new} \mathcal{R}u)(n_1, n_2) &= (\mathcal{R}u)(n_1 + \tfrac{1}{2}, n_2) - (\mathcal{R}u)(n_1 - \tfrac{1}{2}, n_2) = u(n_2, N_2 + 1 - n_1 - \tfrac{1}{2}) - u(n_2, N_2 + 1 - n_1 + \tfrac{1}{2}) \\ &= -(\mathcal{D}_{y_\bullet}^{new} u)(n_2, N_2 + 1 - n_1) = -(\mathcal{R} \mathcal{D}_{y_\bullet}^{new} u)(n_1, n_2), \end{aligned} \quad (54)$$

for $\frac{3}{2} \leq n_1 \leq N_2 - \frac{1}{2}$, $1 \leq n_2 \leq N_1$. Also considering the boundary cases, it is easy to conclude that $\mathcal{D}_{x_\bullet}^{new} \mathcal{R} = -\mathcal{R} \mathcal{D}_{y_\bullet}^{new}$. Likewise,

$$\begin{aligned} (\mathcal{D}_{y_\bullet}^{new} \mathcal{R}u)(n_1, n_2) &= (\mathcal{R}u)(n_1, n_2 + \tfrac{1}{2}) - (\mathcal{R}u)(n_1, n_2 - \tfrac{1}{2}) = u(n_2 + \tfrac{1}{2}, N_2 + 1 - n_1) - u(n_2 - \tfrac{1}{2}, N_2 + 1 - n_1) \\ &= (\mathcal{D}_{x_\bullet}^{new} u)(n_2, N_2 + 1 - n_1) = (\mathcal{R} \mathcal{D}_{x_\bullet}^{new} u)(n_1, n_2), \end{aligned} \quad (55)$$

for $1 \leq n_1 \leq N_2$, $\frac{3}{2} \leq n_2 \leq N_1 - \frac{1}{2}$, allowing us to conclude analogously that $\mathcal{D}_{y_\bullet}^{new} \mathcal{R} = \mathcal{R} \mathcal{D}_{x_\bullet}^{new}$. Thus, with the linear isomorphism $\bar{\mathcal{R}} : \mathcal{U}_{\leftrightarrow} \times \mathcal{U}_\uparrow \rightarrow \mathcal{U}_{\leftrightarrow}^\perp \times \mathcal{U}_\uparrow^\perp$ according to $\bar{\mathcal{R}}(w_1, w_2) = (-\mathcal{R}w_2, \mathcal{R}w_1)$, we have $\mathcal{D}^{new} \mathcal{R} = \bar{\mathcal{R}} \mathcal{D}^{new}$.

Considerations that are completely analogous also lead to the identities $\mathcal{D}_{x_\star}^{new} \mathcal{R} = -\mathcal{R} \mathcal{D}_{y_\star}^{new}$, $\mathcal{D}_{y_\star}^{new} \mathcal{R} = \mathcal{R} \mathcal{D}_{x_\star}^{new}$ for $u \in \mathcal{U}_\star$, $\star = \leftrightarrow, \uparrow$. Thus, for $w \in \mathcal{U}_{\leftrightarrow} \times \mathcal{U}_\uparrow$ we see that

$$\mathcal{E}^{new} \bar{\mathcal{R}}w = \begin{pmatrix} \mathcal{R} \mathcal{D}_{y_\uparrow}^{new} w_2 \\ \mathcal{R} \mathcal{D}_{x_{\leftrightarrow}}^{new} w_1 \\ -\frac{1}{2}(\mathcal{R} \mathcal{D}_{x_\uparrow}^{new} w_2 + \mathcal{R} \mathcal{D}_{y_{\leftrightarrow}}^{new} w_1) \end{pmatrix} = \bar{\mathcal{R}} \mathcal{E}^{new} w, \quad (56)$$

where the linear isomorphism $\bar{\mathcal{R}} : \mathcal{U}_\bullet^x \times \mathcal{U}_\bullet^y \times \mathcal{U}_\times \rightarrow \mathcal{U}_\bullet^{x\perp} \times \mathcal{U}_\bullet^{y\perp} \times \mathcal{U}_\times^\perp$ is given by $\bar{\mathcal{R}} = (\mathcal{R}v_2, \mathcal{R}v_1, -\mathcal{R}v_3)$.

Let us now discuss how the operators L_\star^* , $\star = \bullet, \leftrightarrow, \uparrow$ behave under rotation. For instance, for $w_\bullet \in \mathcal{U}_\bullet \times \mathcal{U}_\bullet$ we have

$$(\bar{\mathcal{R}} L_\bullet^* w_\bullet)(n_1, n_2) = \begin{pmatrix} -\frac{1}{2}(w_\bullet^2(n_2 + \tfrac{1}{2}, N_2 + 1 - n_1) + w_\bullet^2(n_2 - \tfrac{1}{2}, N_2 + 1 - n_1)) \\ \frac{1}{2}(w_\bullet^1(n_2, N_2 + 1 - n_1 - \tfrac{1}{2}) + w_\bullet^1(n_2, N_2 + 1 - n_1 + \tfrac{1}{2})) \end{pmatrix} = (L_\bullet^* \bar{\mathcal{R}} w_\bullet)(n_1, n_2) \quad (57)$$

for $\frac{3}{2} \leq n_1 \leq N_2 - \frac{1}{2}$, $\frac{3}{2} \leq n_2 \leq N_1 - \frac{1}{2}$ where $\bar{\mathcal{R}}$ on the right-hand side has to be understood, analogous to the above, as a mapping $\mathcal{U}_\bullet \times \mathcal{U}_\bullet \rightarrow \mathcal{U}_\bullet^\perp \times \mathcal{U}_\bullet^\perp$. Taking also the boundary cases into account, we are able to conclude that $\bar{\mathcal{R}} L_\bullet^* = L_\bullet^* \bar{\mathcal{R}}$. With the same reasoning, we also get that $\bar{\mathcal{R}} L_{\leftrightarrow}^* = L_{\leftrightarrow}^* \bar{\mathcal{R}}$ as well as $\bar{\mathcal{R}} L_\uparrow^* = L_\uparrow^* \bar{\mathcal{R}}$. This also applies to L_\bullet^* given for $v \in \mathcal{U}_\bullet \times \mathcal{U}_\bullet \times \mathcal{U}_\bullet$ for which the identity $\bar{\mathcal{R}} L_\bullet^* = L_\bullet^* \bar{\mathcal{R}}$ holds for $\bar{\mathcal{R}}$ on the right-hand side mapping $\mathcal{U}_\bullet \times \mathcal{U}_\bullet \times \mathcal{U}_\bullet \rightarrow \mathcal{U}_\bullet^\perp \times \mathcal{U}_\bullet^\perp \times \mathcal{U}_\bullet^\perp$.

For the $u \in \mathcal{U}_\bullet$ given in the statement of the theorem, consider $(v_\bullet, w_\bullet, w_{\leftrightarrow}, w_\uparrow, \omega)$ as well as

$$(v_\bullet^\perp, w_\bullet^\perp, w_{\leftrightarrow}^\perp, w_\uparrow^\perp, \omega^\perp) = (\bar{\mathcal{R}} v_\bullet, \bar{\mathcal{R}} w_\bullet, \bar{\mathcal{R}} w_\uparrow, \bar{\mathcal{R}} w_{\leftrightarrow}, \bar{\mathcal{R}} \omega). \quad (58)$$

Now, using the above identities, we can see that

$$\begin{aligned} \mathcal{D}^{new}u - \omega &= L_{\bullet}^*w_{\bullet} + L_{\leftrightarrow}^*w_{\leftrightarrow} + L_{\updownarrow}^*w_{\updownarrow} & \Leftrightarrow & \bar{\mathcal{R}}\mathcal{D}^{new}u - \bar{\mathcal{R}}\omega = \bar{\mathcal{R}}L_{\bullet}^*w_{\bullet} + \bar{\mathcal{R}}L_{\leftrightarrow}^*w_{\leftrightarrow} + \bar{\mathcal{R}}L_{\updownarrow}^*w_{\updownarrow} \\ \Leftrightarrow \mathcal{D}^{new}\mathcal{R}u - \bar{\mathcal{R}}\omega &= L_{\bullet}^*\bar{\mathcal{R}}w_{\bullet} + L_{\updownarrow}^*\bar{\mathcal{R}}w_{\leftrightarrow} + L_{\leftrightarrow}^*\bar{\mathcal{R}}w_{\updownarrow} & \Leftrightarrow & \mathcal{D}^{new}\mathcal{R}u - \omega^{\perp} = L_{\bullet}^*w_{\bullet}^{\perp} + L_{\leftrightarrow}^*w_{\leftrightarrow}^{\perp} + L_{\updownarrow}^*w_{\updownarrow}^{\perp}, \end{aligned} \quad (59)$$

as well as

$$\mathcal{E}^{new}\omega = L_{\bullet}^*v_{\bullet} \quad \Leftrightarrow \quad \bar{\mathcal{R}}\mathcal{E}^{new}\omega = \bar{\mathcal{R}}L_{\bullet}^*v_{\bullet} \quad \Leftrightarrow \quad \mathcal{E}^{new}\bar{\mathcal{R}}\omega = L_{\bullet}^*\bar{\mathcal{R}}v_{\bullet} \quad \Leftrightarrow \quad \mathcal{E}^{new}\omega^{\perp} = L_{\bullet}^*v_{\bullet}^{\perp}. \quad (60)$$

Consequently, $(v_{\bullet}, w_{\bullet}, w_{\leftrightarrow}, w_{\updownarrow}, \omega)$ is feasible for (48) if and only if $(v_{\bullet}^{\perp}, w_{\bullet}^{\perp}, w_{\leftrightarrow}^{\perp}, w_{\updownarrow}^{\perp}, \omega^{\perp})$ is feasible for (48) with u replaced by the rotated image $\mathcal{R}u$. Finally, it is easy to see that $\bar{\mathcal{R}}$ and $\bar{\mathcal{R}}$ preserve the 1-norm such that

$$\alpha_0\|v_{\bullet}\|_1 + \alpha_1\|w_{\bullet}\|_1 + \alpha_1\|w_{\leftrightarrow}\|_1 + \alpha_1\|w_{\updownarrow}\|_1 = \alpha_0\|v_{\bullet}^{\perp}\|_1 + \alpha_1\|w_{\bullet}^{\perp}\|_1 + \alpha_1\|w_{\leftrightarrow}^{\perp}\|_1 + \alpha_1\|w_{\updownarrow}^{\perp}\|_1. \quad (61)$$

With the latter three statements, i.e., (59), (60) and (61), the identity $\text{TGV}_{\alpha}^{2(new)}(u) = \text{TGV}_{\alpha}^{2(new)}(\mathcal{R}u)$ then follows directly from (48). \square

5. Numerical algorithms and application to denoising

In the following, we propose numerical algorithms associated with the proposed discrete TGV for solving denoising problems and the computation of the TGV value. We compare the denoising results with some discrete variational models. Moreover, for some test images and their 90° rotated versions, the value of the TGV for the proposed model and the classic discrete TGV are computed and compared.

5.1. Denoising

Here, we consider the denoising problem and evaluate our proposed discrete TGV and compare it with classic discrete TV, Condat's TV and the classic discretization of TGV. Consider the general form of the denoising problem

$$\min_{u \in \mathbb{R}^{N_1 \times N_2}} F(u) + R(u), \quad (62)$$

which is the discrete form of the variational problem (1). In this formulation, $F(u) = \frac{1}{2}\|u - f\|^2$ for some noisy image $f \in \mathbb{R}^{N_1 \times N_2}$. Moreover, we can set any discrete total variation model or discrete second-order TGV model for R . We consider the following four denoising problems:

$$\begin{aligned} (a) \text{ Classic TV denoising problem} & \quad \min_u F(u) + \lambda \text{TV}(u), \\ (b) \text{ Condat's TV denoising problem} & \quad \min_u F(u) + \lambda \text{TV}_c(u), \\ (c) \text{ Classic TGV denoising problem} & \quad \min_u F(u) + \text{TGV}_{\alpha}^2(u), \\ (d) \text{ Proposed TGV denoising problem} & \quad \min_u F(u) + \text{TGV}_{\alpha}^{2(new)}(u), \end{aligned} \quad (63)$$

where $\lambda, \alpha_0, \alpha_1 > 0$. As the numerical algorithms for solving problems (63) (a)–(c) already have been studied in the literature, we only focus here on describing a suitable algorithm for solving problem (63) (d). From Theorem 3.8 it is easy to see that problem (63) (d) is equivalent to the following problem:

$$\begin{aligned} \min_{v_{\bullet}, w_{\bullet}, w_{\leftrightarrow}, w_{\updownarrow}, u, \omega} & \quad F(u) + \alpha_0\|v_{\bullet}\|_1 + \alpha_1\|w_{\bullet}\|_1 + \alpha_1\|w_{\leftrightarrow}\|_1 + \alpha_1\|w_{\updownarrow}\|_1 \\ \text{subject to} & \quad \bar{L}^*(v_{\bullet}, w_{\bullet}, w_{\leftrightarrow}, w_{\updownarrow}, u, \omega)^T = 0, \end{aligned} \quad (64)$$

where $\bar{L}^* = \begin{pmatrix} L_{\bullet}^* & 0 & 0 & 0 & 0 & -\mathcal{E}^{new} \\ 0 & L_{\bullet}^* & L_{\leftrightarrow}^* & L_{\updownarrow}^* & -\mathcal{D}^{new} & I \end{pmatrix}$. In the numerical experiments below, we employ the Chambolle–Pock algorithm [33] (see Algorithm 1). The algorithm generally can be used to solve the following optimization problem:

$$\min_z \mathcal{F}(Az) + \mathcal{G}(z), \quad (65)$$

Data: $A, A^*, \mathcal{F}^*, \mathcal{G}$

Result: For iteration number N , z^N primal solution approximation and y^N dual solution approximation

Initialization: Choose parameters $\sigma > 0, \tau > 0$ with $\sigma\tau\|A\|^2 < 1$ and initial estimates $(z^0, y^0) \in X \times Y, \tilde{z}^0 = z^0$

while convergence criterion not met, for $k=0, 1, \dots$ **do**

$$\begin{cases} y^{k+1} = \text{prox}_{\sigma\mathcal{F}^*}(y^k + \sigma A\tilde{z}^k) \\ z^{k+1} = \text{prox}_{\tau\mathcal{G}}(z^k - \tau A^*y^{k+1}) \\ \tilde{z}^{k+1} = 2z^{k+1} - z^k \end{cases}$$

end

Algorithm 1: The Chambolle–Pock algorithm for solving problem (65).

and its dual form

$$\min_y \mathcal{F}^*(y) + \mathcal{G}^*(-A^*y), \quad (66)$$

where $A : X \rightarrow Y$ is a linear and continuous operator, $\mathcal{F} : Y \rightarrow]-\infty, \infty]$ and $\mathcal{G} : X \rightarrow]-\infty, \infty]$ are proper, convex and lower semi-continuous functions whose corresponding proximal operators have simple forms or can easily be calculated. The algorithm is guaranteed to converge to a primal-dual solution pair provided that a primal-dual solution exists, there is no duality gap and that $\sigma > 0, \tau > 0$ satisfy $\sigma\tau < \frac{1}{\|A\|^2}$. In practical situations where computing the exact value of $\|A\|$ is difficult, finding an upper bound $B > \|A\|^2$ and setting $\sigma = \tau = \frac{1}{\sqrt{B}}$ is sufficient for convergence. In our case, for the denoising problem, we choose $F(u) = \frac{1}{2}\|u - f\|_2^2$ for a noisy image $f \in \mathcal{U}_\bullet$ and

$$\begin{aligned} z &= (v_\bullet, w_\bullet, w_\leftrightarrow, w_\updownarrow, u, \omega) \in X = \mathcal{U}_\bullet^3 \times \mathcal{U}_\bullet^2 \times \mathcal{U}_\leftrightarrow^2 \times \mathcal{U}_\updownarrow^2 \times \mathcal{U}_\bullet \times (\mathcal{U}_\leftrightarrow \times \mathcal{U}_\updownarrow), \\ \mathcal{G}(z) &= F(u) + \alpha_0\|v_\bullet\|_1 + \alpha_1\|w_\bullet\|_1 + \alpha_1\|w_\leftrightarrow\|_1 + \alpha_1\|w_\updownarrow\|_1. \end{aligned}$$

Furthermore, set $A = \bar{L}$, the adjoint of the operator \bar{L}^* defined above and

$$y = \begin{pmatrix} v \\ w \end{pmatrix} \in Y = (\bar{\mathcal{U}}_\bullet^x \times \bar{\mathcal{U}}_\bullet^v \times \mathcal{U}_\times) \times (\mathcal{U}_\leftrightarrow \times \mathcal{U}_\updownarrow), \quad \mathcal{F}(y) = I_{\{0\}}(y).$$

It is not difficult to see that

$$\text{prox}_{\sigma\mathcal{F}^*}(\gamma) = \gamma, \quad \gamma \in Y.$$

Moreover, it is well known that

$$\text{prox}_{\tau\|\cdot\|_1}(w)(n_1, n_2) = \text{shrink}_\tau(w)(n_1, n_2) = \left(1 - \frac{\tau}{\max\{|w(n_1, n_2)|, \tau\}}\right)w(n_1, n_2),$$

for $w \in \mathcal{U}_\star \times \mathcal{U}_\star, \star = \bullet, \leftrightarrow, \updownarrow$ where $|w(n_1, n_2)| = \sqrt{w^1(n_1, n_2)^2 + w^2(n_1, n_2)^2}$. The proximal mapping of $\tau\|\cdot\|_1$ for $v \in \mathcal{U}_\bullet \times \mathcal{U}_\bullet \times \mathcal{U}_\bullet$ is given analogously with $|v(n_1, n_2)| = \sqrt{v^1(n_1, n_2)^2 + v^2(n_1, n_2)^2 + 2v^3(n_1, n_2)^2}$. It can easily be verified that $\text{prox}_{\tau\mathcal{G}}(v_\bullet, w_\bullet, w_\leftrightarrow, w_\updownarrow, u, \omega) = (\bar{v}_\bullet, \bar{w}_\bullet, \bar{w}_\leftrightarrow, \bar{w}_\updownarrow, \bar{u}, \bar{\omega})$ where

$$\bar{v}_\bullet = \text{shrink}_{\alpha_0\tau}(v_\bullet), \quad \bar{w}_\star = \text{shrink}_{\alpha_1\tau}(w_\star), \star = \bullet, \leftrightarrow, \updownarrow, \quad \bar{u} = \frac{u + \tau f}{1 + \tau}, \quad \bar{\omega} = \omega. \quad (67)$$

Based on above functionals and parameters, Algorithm 2 is proposed to solve the denoising problem (64) as well as its dual form which can equivalently be written as the following optimization problem:

$$\begin{aligned} \min_{v, w} \quad & \frac{1}{2}\|\text{div}^{new} w\|_2^2 + \langle \text{div}^{new} w, f \rangle \\ \text{subject to} \quad & \begin{cases} \|L_\bullet v\|_\infty \leq \alpha_0, \\ \|L_\star w\|_\infty \leq \alpha_1, \star = \bullet, \leftrightarrow, \updownarrow, \\ w = \text{div}^{new} v. \end{cases} \end{aligned} \quad (68)$$

We also applied the three different variational models (63) (a)–(c) to solve the image denoising problem (see the

Data: Noisy image $f \in \mathcal{U}_\bullet$, $\alpha = (\alpha_0, \alpha_1)$, $\alpha_0 > 0, \alpha_1 > 0$

Result: For the iteration number N , $z^N = (v_\bullet^N, w_\bullet^N, w_{\leftrightarrow}^N, w_{\updownarrow}^N, u^N, \omega^N)$, is an approximation of the solution of the primal problem (64) and u^N is the obtained denoised image. Moreover, $y^N = (v^N, w^N)$ is an approximation of a solution of the dual problem (68)

Initialization:

Choose $\sigma > 0$ and $\tau > 0$ such that $\sigma\tau\|\bar{L}\|^2 < 1$

Choose the initial approximation $u^0 = \tilde{u}^0 = f \in \mathcal{U}_\bullet$

Choose an arbitrary initial approximation of a primal solution $v_\bullet^0 = \tilde{v}_\bullet^0 \in \mathcal{U}_\bullet \times \mathcal{U}_\bullet \times \mathcal{U}_\bullet$,

$w_\star^0 = \tilde{w}_\star^0 \in \mathcal{U}_\star \times \mathcal{U}_\star$, $\star = \bullet, \leftrightarrow, \updownarrow$, $\omega^0 = \tilde{\omega}^0 \in \mathcal{U}_{\leftrightarrow} \times \mathcal{U}_{\updownarrow}$

Choose an arbitrary initial approximation of a dual solution $v^0 \in \tilde{\mathcal{U}}_\bullet^x \times \tilde{\mathcal{U}}_\bullet^y \times \mathcal{U}_x$, $w^0 \in \mathcal{U}_{\leftrightarrow} \times \mathcal{U}_{\updownarrow}$

while convergence criterion not met, for $k = 0, 1, \dots$ **do**

$$\begin{aligned} v_\bullet^{k+1} &= v_\bullet^k + \sigma(L_\bullet^* \tilde{v}_\bullet^k - \mathcal{E}^{new} \tilde{\omega}^k) \\ w_\star^{k+1} &= w_\star^k + \sigma(L_\star^* \tilde{w}_\star^k + L_{\leftrightarrow}^* \tilde{w}_{\leftrightarrow}^k + L_{\updownarrow}^* \tilde{w}_{\updownarrow}^k - \mathcal{D}^{new} \tilde{u}^k + \tilde{\omega}^k) \\ v_\bullet^{k+1} &= \text{shrink}_{\alpha_0 \tau}(v_\bullet^k - \tau L_\bullet v_\bullet^{k+1}), w_\star^{k+1} = \text{shrink}_{\alpha_1 \tau}(w_\star^k - L_\star w_\star^{k+1}), \star = \bullet, \leftrightarrow, \updownarrow \\ u^{k+1} &= \frac{u^k - \tau(\text{div}^{new} w_\star^{k+1} - f)}{1 + \tau}, \omega^{k+1} = \omega^k - \tau(\text{div}^{new} v_\bullet^{k+1} + w_\star^{k+1}) \\ \tilde{v}_\bullet^{k+1} &= 2v_\bullet^{k+1} - v_\bullet^k, \tilde{w}_\star^{k+1} = 2w_\star^{k+1} - w_\star^k, \star = \bullet, \leftrightarrow, \updownarrow \\ \tilde{u}^{k+1} &= 2u^{k+1} - u^k, \tilde{\omega}^{k+1} = 2\omega^{k+1} - \omega^k \end{aligned}$$

end

Algorithm 2: An algorithm for solving problem (64) and its dual form (68).

reference images in Figure 3) and compare the results with the newly proposed discrete TGV (problem (63) (d)). The parameters of each model are optimized to achieve the best reconstruction with respect to peak signal to noise ratio (PSNR). In the algorithms we need the two parameters $\sigma > 0$ and $\tau > 0$ to satisfy $\sigma\tau\|\bar{L}\|^2 < 1$. For classical discrete TV and Condat's TV, we set $\tau = \frac{0.99}{8}, \sigma = \frac{0.99}{3}$ as recommended in [11] and for both discrete TGV models, we set $\tau = \sigma = \frac{5}{37}$ and for all simulations, the number of iterations is $N = 500$. For the images, whose intensity values are stored as double-precision float-point numbers in the range $[0, 1]$, we artificially produce a noisy image by adding Gaussian noise with 0 mean and standard deviation 0.1 to the respective clean image.

We consider two criteria to compare the results; accuracy and the ability to remove artifacts (especially, the staircase effect). In [11], Condat shows that the discrete total variation model developed in this work has better quality in terms of accuracy and isotropy in comparison to state-of-the-art discrete total variation models. Moreover, classic discrete TGV [13] is a variational model whose experimental results show that it is very efficient in sense of reducing artifacts such as the staircase effect.

Numerical results (Table 1) confirm that the proposed model can restore images with better accuracy (PSNR and SSIM [34] values) whereas staircase artifacts are more attenuated (see Figures 4–7). That is, the new proposed TGV is more accurate in comparison to Condat's TV and preserves the artifact-reducing property of the discrete classic second-order TGV (see again Figures 4–7). The resulting images are cleaner from noise and the PSNR and SSIM values are the highest in comparison to the other variational models. To observe more details of the reconstructed images, parts of the obtained images are also shown in a zoomed version in the figures.

5.2. Computation of TGV; classic TGV vs. proposed TGV

In this section the rotational invariance property of the classic discrete TGV and the proposed discrete TGV are compared. For three test images (see Figure 8), the classic discrete TGV values and the proposed discrete TGV values of the images as well as their 90° rotated versions are calculated.

To compute an approximation of the classic discrete TGV and the proposed one, we solve the optimization problems (51) and (52), respectively, by means of the primal-dual algorithm (Algorithm 1). In order to solve (52), let

$$\tilde{L}^* = \begin{pmatrix} L_\bullet^* & 0 & 0 & 0 & -\mathcal{E}^{new} \\ 0 & L_\bullet^* & L_{\leftrightarrow}^* & L_{\updownarrow}^* & I \end{pmatrix}. \text{ Then, we can rewrite the constraint of (52) as}$$

$$\tilde{L}^*(v_\bullet, w_\bullet, w_{\leftrightarrow}, w_{\updownarrow}, \omega)^T = (0, \mathcal{D}^{new} u)^T.$$

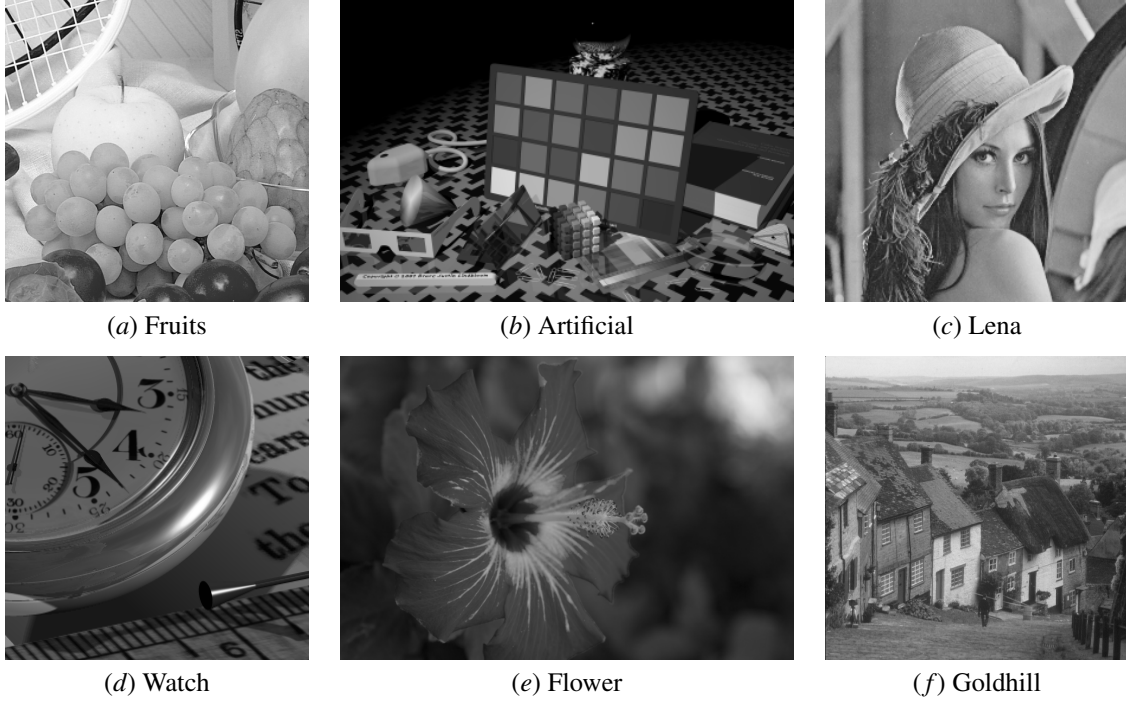


Figure 3: Reference images: gray scaled images in “png” format with the following sizes: (a) Fruits (512×512 pixels), (b) Artificial (384×256 pixels), (c) Lena (256×256 pixels), (d) Watch (300×300 pixels), (e) Flower (567×378 pixels) and (f) Goldhill (512×512 pixels).

Now, set

$$z = (v_\bullet, w_\bullet, w_{\leftrightarrow}, w_{\updownarrow}, \omega)^T, \quad \mathcal{G}(z) = \alpha_0 \|v_\bullet\|_1 + \alpha_1 \sum_{\star=\bullet, \leftrightarrow, \updownarrow} \|w_\star\|_1, \quad y = \begin{pmatrix} v \\ w \end{pmatrix}, \quad \mathcal{F}(y) = I_{\{(0, \mathcal{D}^{new} u)\}}(y), \quad A = \tilde{L}^*.$$

Then, problem (52) can be written in terms of (65). In order to employ Algorithm 1, note that the proximal operators for $\sigma\mathcal{F}^*$ and $\tau\mathcal{G}$ read as:

$$\text{prox}_{\sigma\mathcal{F}^*}(v, w) = (v, w - \sigma\mathcal{D}^{new}u), \quad \text{prox}_{\tau\mathcal{G}}(v_\bullet, w_\bullet, w_{\leftrightarrow}, w_{\updownarrow}, \omega) = (\bar{v}_\bullet, \bar{w}_\bullet, \bar{w}_{\leftrightarrow}, \bar{w}_{\updownarrow}, \bar{\omega}),$$

using the notation of (67). As a result, the primal-dual algorithm to solve (52) is outlined in Algorithm 3. We employed Algorithm 3 with 1000 iterations in our simulations. Table 2 confirms that the proposed TGV has invariant values, up to numerical precision, for the original images and their 90 degree rotated versions.

6. Conclusion

In this paper, the idea of Condat’s discrete total variation’s is transferred to the second-order TGV. A new discrete second-order TGV model is designed based on the building blocks containing the definition of suitable grids, introducing new discrete derivative and divergence operators and proposing suitable linear conversion operators to guarantee some invariance properties. The proposed model is invariant with respect to 90° rotations and shows the benefits of Condat’s discrete TV model. Moreover, the new discrete TGV preserves the ability of the classic discrete TGV to diminish artifacts such as staircase artifacts, which are typical for discrete TV models. The same design principles can be applied for higher-order TGV or in higher dimensions to gain better results for imaging problems. While this can quite easily be done for specific cases, the development of a general framework requires some effort and can thus be regarded a subject of future work.

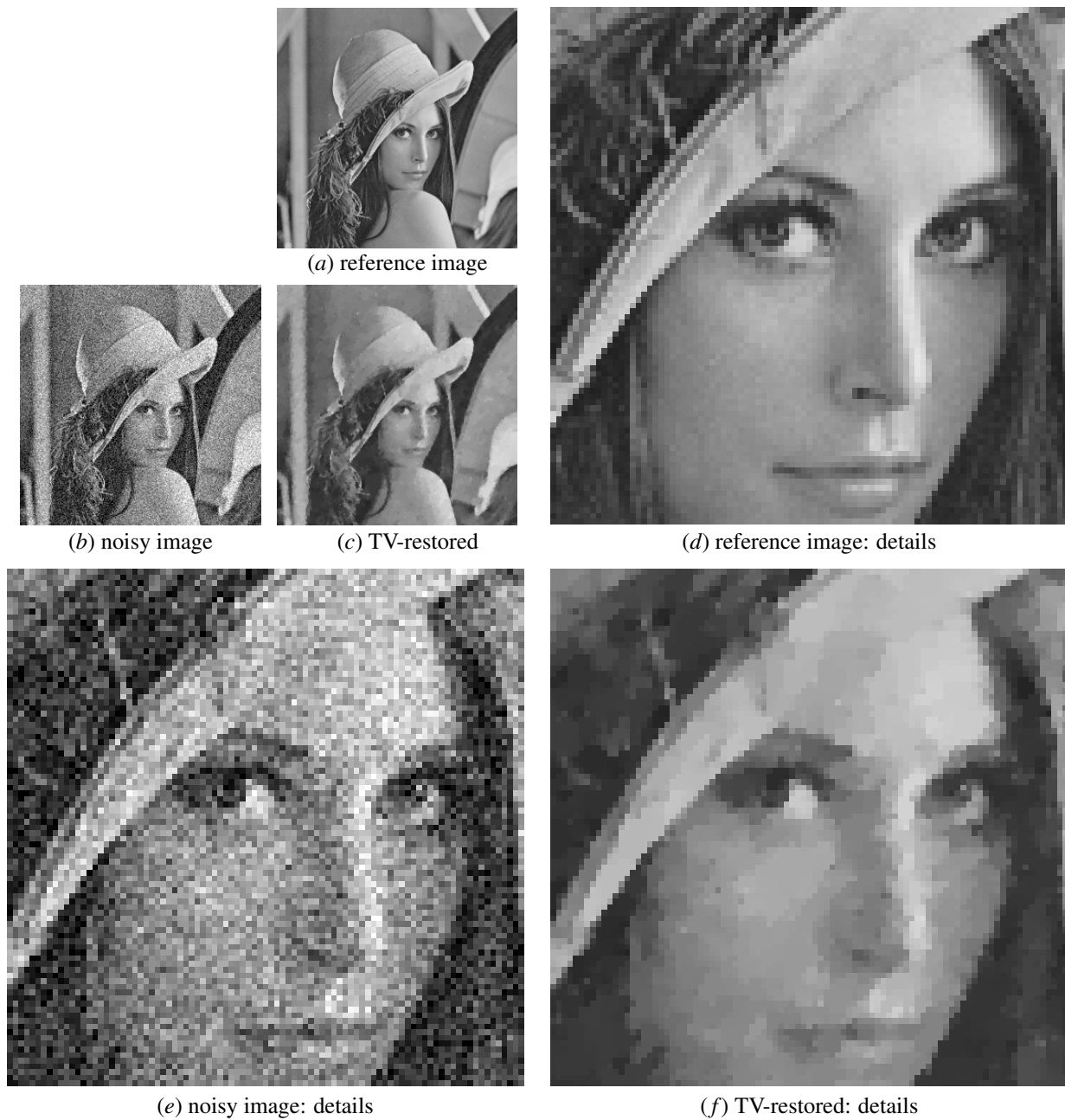


Figure 4: Denoising experiment for the test image “Lena”: reference image, noisy image and restored image using the classic discrete TV model are shown in (a), (b) and (c), respectively. Some details of the reference and noisy image are shown in (d) and (e). The details of the restored image using the classic discrete TV model is shown in (f), where strong staircase artifacts around the interfaces are evident.

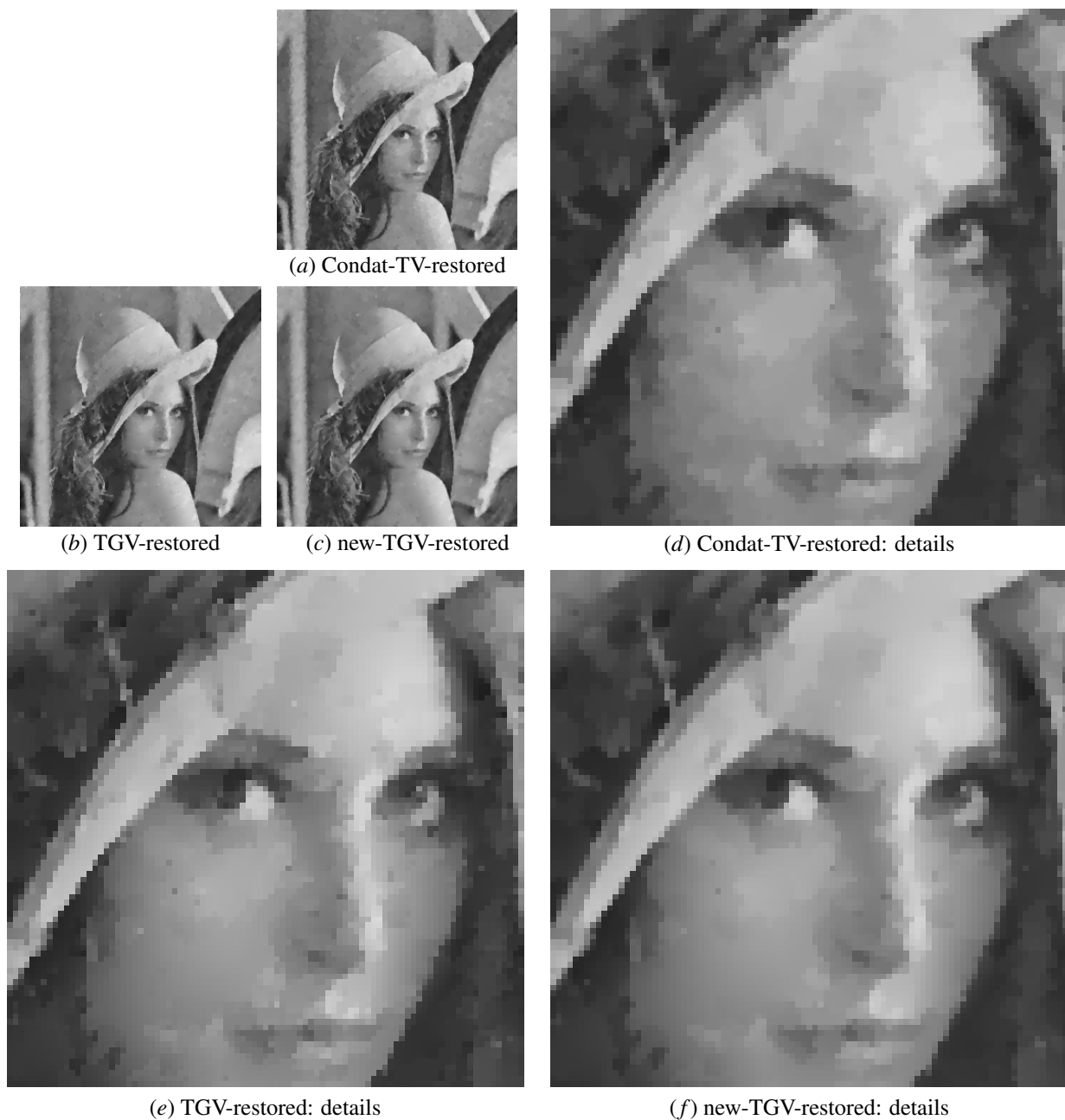


Figure 5: Denoising experiment for the test image “Lena”: the restored images using Condat’s model, the second-order classic discrete TGV model and the proposed model are shown in (a), (b) and (c), respectively. Some details are shown in (d), (e) and (f). The obtained images by means of the TGV models are far better than the restored image using Condat’s TV model in terms of reducing staircase artifacts (for instance, look at the cheeks, in the restored images). In the result for classic discrete TGV, some unwanted narrow edges and speckles are visible in the smooth parts, whereas, in the proposed model, these kinds of effects have decreased significantly. On the other hand, the amount of noise in the image has been reduced using the proposed model. These distinguishing properties, beside the quantitative results (Table 1) show the benefits of the proposed method.

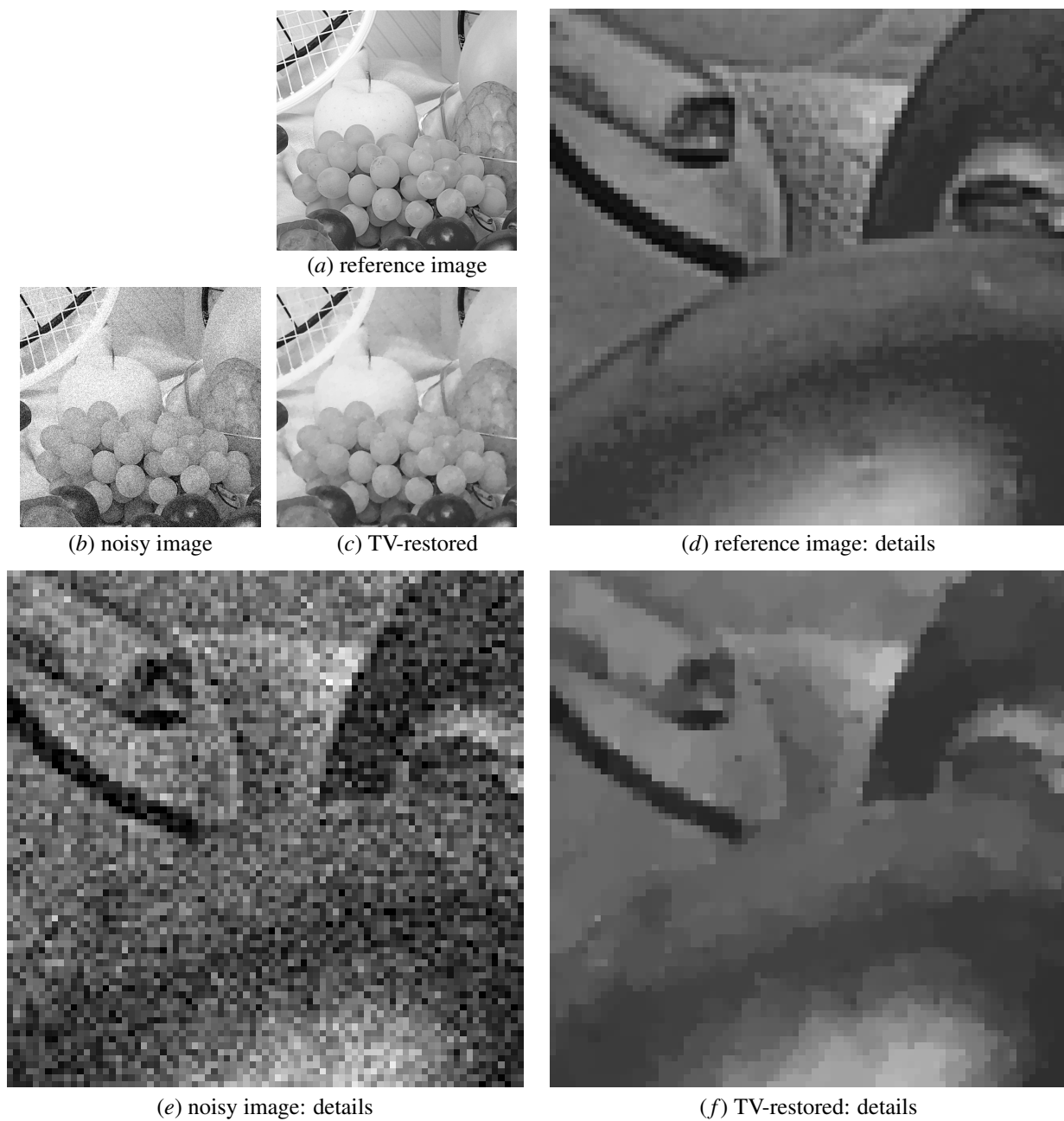


Figure 6: Denoising experiment for the test image “Fruits”: reference image, noisy image and restored image using the classic discrete TV model are shown in (a), (b) and (c), respectively. Some details of the reference and noisy image are shown in (d) and (e). The details of restored image using the classic discrete TV model is shown in (f).

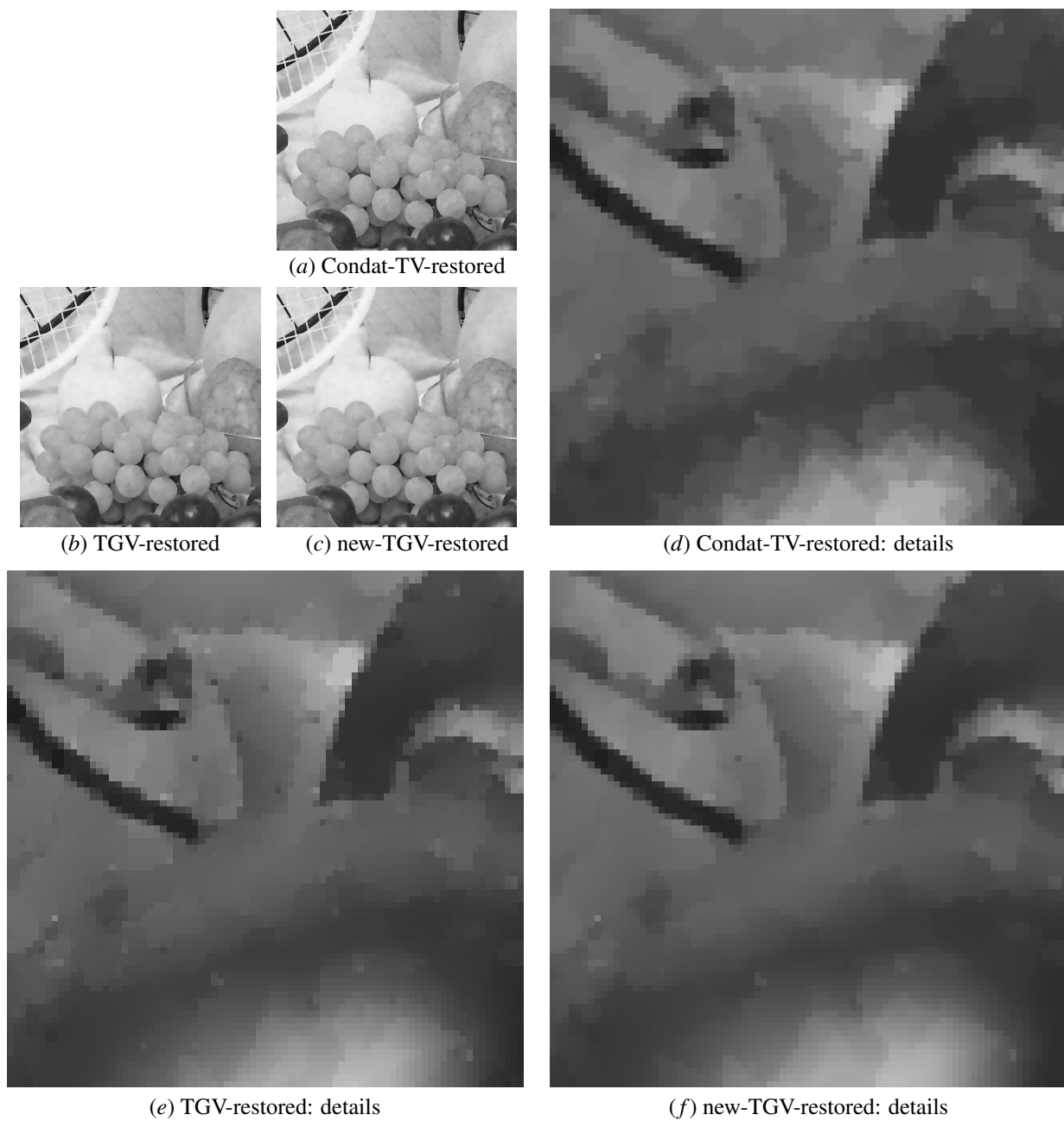


Figure 7: Denoising experiment for the test image “Fruits”: the restored images using Condat’s TV model, the classic second-order discrete TGV model and the proposed model are shown in (a), (b) and (c), respectively. Some details are shown in (d), (e) and (f). The benefits of the proposed model are also evident in this experiment.

Data: Image $u \in \mathcal{U}_\bullet$, $\alpha = (\alpha_0, \alpha_1)$, $\alpha_0 > 0, \alpha_1 > 0$

Result: For the iteration number N , $z^N = (v_\bullet^N, w_\bullet^N, w_{\leftrightarrow}^N, w_{\updownarrow}^N, \omega^N)$, is an approximation of the solution of the primal problem (52). Moreover, $y^N = (v^N, w^N)$ is an approximation of a solution of the dual problem (38) and the approximated new discrete TGV value is $\alpha_0 \|v_\bullet\|_1 + \alpha_1 \sum_{\star=\bullet, \leftrightarrow, \updownarrow} \|w_\star\|_1$

Initialization:

Choose $\sigma > 0$ and $\tau > 0$ such that $\sigma\tau\|\tilde{L}\|^2 < 1$

Choose an arbitrary initial approximation of a primal solution $v_\bullet^0 = \tilde{v}_\bullet^0 \in \mathcal{U}_\bullet \times \mathcal{U}_\bullet \times \mathcal{U}_\bullet$,

$w_\star^0 = \tilde{w}_\star^0 \in \mathcal{U}_\star \times \mathcal{U}_\star$, $\star = \bullet, \leftrightarrow, \updownarrow$, $\omega^0 = \tilde{\omega}^0 \in \mathcal{U}_{\leftrightarrow} \times \mathcal{U}_{\updownarrow}$

Choose an arbitrary initial approximation of a dual solution $v^0 \in \tilde{\mathcal{U}}_\bullet^x \times \tilde{\mathcal{U}}_\bullet^y \times \mathcal{U}_x$, $w^0 \in \mathcal{U}_{\leftrightarrow} \times \mathcal{U}_{\updownarrow}$

while convergence criterion not met, for $k = 0, 1, \dots$ **do**

$v_\bullet^{k+1} = v_\bullet^k + \sigma(L_\bullet^* \tilde{v}_\bullet^k - \mathcal{E}^{new} \tilde{\omega}^k)$

$w_\star^{k+1} = w_\star^k + \sigma(L_\star^* \tilde{w}_\star^k + L_{\leftrightarrow}^* \tilde{w}_{\leftrightarrow}^k + L_{\updownarrow}^* \tilde{w}_{\updownarrow}^k - \mathcal{D}^{new} u + \tilde{\omega}^k)$

$v_\bullet^{k+1} = \text{shrink}_{\alpha_0 \tau}(v_\bullet^k - \tau L_\bullet v_\bullet^{k+1})$, $w_\star^{k+1} = \text{shrink}_{\alpha_1 \tau}(w_\star^k - L_\star w_\star^{k+1})$, $\star = \bullet, \leftrightarrow, \updownarrow$

$\omega^{k+1} = \omega^k - \tau(\text{div}^{new} v_\bullet^{k+1} + w_\star^{k+1})$

$\tilde{v}_\bullet^{k+1} = 2v_\bullet^{k+1} - v_\bullet^k$, $\tilde{w}_\star^{k+1} = 2w_\star^{k+1} - w_\star^k$, $\star = \bullet, \leftrightarrow, \updownarrow$, $\tilde{\omega}^{k+1} = 2\omega^{k+1} - \omega^k$

end

Algorithm 3: An algorithm for solving problem (52) and its dual form (38).



(a) Fruits



(b) Barbara



(c) Bike

Figure 8: The test images used for the 90° isotropy testing problem. From left to right: Fruits, Barbara and Bike test image.

Image	Fruits			Watch			Lena		
Metric	λ^*	PSNR	SSIM	λ^*	PSNR	SSIM	λ^*	PSNR	SSIM
TV	0.080	30.15	0.8006	0.072	28.50	0.8048	0.074	27.85	0.7785
Condat	0.076	30.37	0.8080	0.066	28.80	0.8158	0.068	27.98	0.7832
TGV	0.080	30.21	0.8063	0.072	28.58	0.8101	0.074	27.97	0.7869
Proposed	0.076	30.42	0.8127	0.066	28.87	0.8203	0.068	28.08	0.7902
Image	Artificial			Flower			Goldhill		
Metric	λ^*	PSNR	SSIM	λ^*	PSNR	SSIM	λ^*	PSNR	SSIM
TV	0.064	26.81	0.6273	0.088	33.36	0.8923	0.076	28.57	0.7284
Condat	0.058	27.04	0.6354	0.082	33.55	0.8963	0.070	28.71	0.7350
TGV	0.064	26.82	0.6275	0.088	33.75	0.9104	0.074	28.62	0.7304
Proposed	0.058	27.05	0.6355	0.082	33.90	0.9126	0.068	28.75	0.7367

Table 1: Denoising problem results: the optimal regularization parameters λ^* as well as the best PSNR and SSIM values for denoising of the test images are shown. Note that λ^* is the best parameter λ for the classic discrete TV model and Condat’s TV model for solving the denoising problems (63) (a), (b) while for both TGV models, $\lambda^* = \alpha_1^*$ is the best parameter α_1 , where $\alpha_0 = 2\alpha_1$, $\alpha = (\alpha_0, \alpha_1)$ is chosen for the denoising problems (63) (c), (d).

Image		Fruits		Barbara		Bike	
Model/Rotation		TGV value	Error	TGV value	Error	TGV value	Error
TGV	0°	585.8179	—	1326.9570	—	1720.4858	—
TGV	90°	586.9604	1.1424	1329.7192	2.7621	1706.1505	14.3353
New TGV	0°	630.7414	—	1421.8091	—	1806.2396	—
New TGV	90°	630.7414	3.41×10^{-13}	1421.8091	9.09×10^{-13}	1806.2395	6.82×10^{-13}

Table 2: The values of the classic discrete TGV and the proposed discrete TGV for three test images and their 90° rotated versions. Here, “error” is the absolute difference of the classic discrete TGV (proposed discrete TGV) value of the rotated image and the reference image.

Acknowledgment

This work was partially supported by the International Mathematical Union (IMU).

References

- [1] Ghazel, M., Freeman, G.H. and Vrscaj, E.R.: Fractal image denoising, IEEE Transactions on Image Processing, 12, 1560–1578 (2003).
- [2] Buades, A., Coll, B. and Morel, J.M.: Image denoising methods. A new nonlocal principle, SIAM Rev., 52, 113–147 (2010).
- [3] Wen, Y.W., Michael, K.N. and Ching, W.K.: Iterative algorithms based on decoupling of deblurring and denoising for image restoration, SIAM J. Sci. Comput., 30, 2655–2674 (2008).
- [4] Sardy, S., Tseng, P. and Bruce, A.: Robust wavelet denoising, IEEE Trans. Sig. Process., 49, 1146–1152 (2001).
- [5] Dabov, K., Foi, A., Katkovnik, V. and Egiazarian, K.: Image denoising by sparse 3-D transform-domain collaborative filtering, IEEE Trans. Image Process., 16, 2080–2095 (2007).
- [6] Perona, P. and Malik, J.: Scale-space and edge detection using anisotropic diffusion, IEEE Trans. Pattern Anal. Mach. Intell., 12, 629–639 (1990).
- [7] Weickert, J.: Anisotropic diffusion in Image Processing, Teubner, Stuttgart, 1998.
- [8] Rudin, L. I., Osher, S., Fatemi, E.: Nonlinear total variation based noise removal algorithms, Phys. D, 60, 259–268 (1992).
- [9] Chambolle, A., Levine, S.E., Lucier, B. J.: An upwind finite-difference method for total variation based image smoothing, SIAM J. Imaging Sci., 4, 277–299 (2011).
- [10] Alter, F., Caselles, V., Chambolle, A.: Evolution of characteristic functions of convex sets in the plane by the minimizing total variation flow, Interfaces Free Bound., 7, 29–53 (2005).
- [11] Condat, L.: Discrete total variation: new definition and minimization, SIAM Journal on Imaging Sciences, 10(3), 1258–1290 (2017).
- [12] Abergel, R., Moisan, L.: The Shannon total variation, J. Math Imaging Vis., 59, 341–370 (2017).
- [13] Bredies, K., Kunisch, K. and Pock, T.: Total generalized variation, SIAM J. Imaging Sci., 3, 492–526 (2010).

- [14] Bredies, K. and Holler, M.: Regularization of linear inverse problems with total generalized variation, *Journal of Inverse and Ill-posed Problems*, 22(6), 871–913 (2014).
- [15] Bredies, K. and Holler, M.: Higher-order total variation approaches and generalisations. *Inverse Problems*, 36(12), 123001, (2020).
- [16] Bredies, K.: Recovering piecewise smooth multichannel images by minimization of convex functionals with total generalized variation penalty. *Lecture Notes in Computer Science*, 8293, 44–77 (2014).
- [17] Valkonen, T., Bredies, K. and Knoll, F.: Total Generalized Variation in Diffusion Tensor Imaging, *SIAM J. Imaging Sci.*, 6(1), 487–525 (2013).
- [18] Papafitsoros, K. and Bredies, K.: A study of the one dimensional total generalised variation regularisation problem. *Inverse Problems and Imaging*, 9(2), 511–550 (2015).
- [19] Bredies, K., Holler, M., Storath, M. and Weinmann, A.: Total Generalized Variation for Manifold-valued Data, *SIAM J. Imaging Sci.*, 11(3), 1785–1848, (2018)
- [20] Knoll, F., Bredies, K., Pock, T. and Stollberger, R.: Second order total generalized variation (TGV) for MRI, *Magnetic Resonance in Medicine*, 65(2), 480–491, (2011).
- [21] Langkammer, C., Bredies, K., Poser, B.A., Barth, M., Reishofer, G., Fan, A.P., Bilgic, B., Fazekas, F., Mainero, C. and Ropele, S.: Fast Quantitative Susceptibility Mapping using 3D EPI and Total Generalized Variation, *NeuroImage*, 111, 622–630 (2015).
- [22] Knoll, F., Holler, M., Koesters, T., Otazo, R., Bredies, C. and Sodickson, D.: Joint MR-PET reconstruction using a multi-channel image regularizer, *IEEE Trans. Med. Image.*, 36(1), 1–16 (2017).
- [23] Huber, R., Haberfehlner, G., Holler, M., Kothleitner, G. and Bredies, K.: Total Generalized Variation regularization for multi-modal electron tomography. *Nanoscale*, 11, 5617–5632, 2019.
- [24] Bredies, K., Nuster, R. and Watschinger, R.: TGV-regularized inversion of the Radon transform for photoacoustic tomography. *Biomedical Optics Express*, 11(2), 994–1019 (2020).
- [25] Bredies, K. and Holler, M.: A TGV-based framework for variational image decompression, zooming and reconstruction. Part I: Analytics. *SIAM J. Imaging Sci.*, 8(4), 2814–2850 (2015).
- [26] Bredies, K. and Holler, M.: A TGV-based framework for variational image decompression, zooming and reconstruction. Part II: Numerics. *SIAM J. Imaging Sci.*, 8(4), 2851–2886 (2015).
- [27] Lore, K.G., Akintayo, A. and Sarkar, S.: LLNET: A deep autoencoder approach to natural low-light image enhancement, *Pattern Recognit.*, 61, 650–662 (2015).
- [28] Wang, N., Tao, D., Gao, X., Li, X. and Li, J.: A comprehensive survey to face hallucination, *Int. J. Comput. Vis.*, 106, 9–30 (2014).
- [29] Hu, Y., Wang, N., Tao, D., Gao, X. and Li, X.: Serf: a simple, effective, robust, and fast image super-resolver from cascaded linear regression, *IEEE Trans. Image Process.*, 25, 4091–4102 (2016).
- [30] Bauschke, H.H., Combettes, P.L.: *Convex Analysis and Monotone Operator Theory in Hilbert Spaces*, 2nd ed. Springer, New York, 2017.
- [31] Chambolle, A., Caselles, V., Cremers, D., Novaga, M. and Pock, T.: An Introduction to Total Variation for Image Analysis, in *Theoretical Foundations and Numerical Methods for Sparse Recovery*, Germany, Berlin: De Gruyter, vol. 9, 263–340, 2010.
- [32] Chambolle, A. and Pock, T.: Crouzeix–Raviart approximation of the total variation on simplicial meshes, *J. Math Imaging Vis.*, 62, 872–899 (2020).
- [33] Chambolle, A. and Pock, T.: A first-order primal-dual algorithm for convex problems with applications to imaging, *J. Math Imaging Vis.*, 40, 120–145 (2011).
- [34] Wang, Z., Bovik, A.C., Sheikh, H.R., Simoncelli, E.P.: Image quality assessment: from error visibility to structural similarity, *IEEE Trans. Image Process.*, 13(4), 600–612 (2004).